Study of nitrogen doped reduced graphene oxide (rGO) for its potential application as a Glucose sensor.

A thesis submitted towards partial fulfillment of the requirements for the degree of:

Master of Technology in Nano Science and Technology

Submitted by:

Koustav Samaddar

Roll no. :002230701017

Registration no. : 163817 of 2022-23

Under the guidance of

Prof.(Dr.) Sourav Sarkar

School of Materials Science and

Nanotechnology

Faculty of Interdisciplinary Studies, Law and Management

Jadavpur

University

Kolkata – 700032

CERTIFICATE OF RECOMMENDATION

This is in order to certify that the thesis entitled "Study of nitrogen doped reduced graphene oxide (rGO) for its potential application as a glucose sensor." is a legitimate work done by Koustav Samaddar under our supervision and guidance for the purposes of fulfilling the requirement for the degree of Master of Technology in Nano Science and Nanotechnology in the School of Materials Science and Nanotechnology from the academic session 2022-2024.

Thesis advisor
Dr Sourav Sarkar
School of Materials Science and Nanotechnology
Jadavpur University,
Kolkata-700 032

Director
School of Materials Science and Nanotechnology
Jadavpur University
Kolkata-700 032

Dean
Faculty Council of Interdisciplinary Studies, Law and Management
Jadavpur University,
Kolkata-700 032

M.Tech (Nano Science and Technology)
Course affiliated to:
Faculty of Interdisciplinary Studies,
Law and Management
Jadavpur University
Kolkata, India

CERTIFICATE OF APPROVAL

I hereby endorse the foregoing thesis as an engineering study, conducted and presented in a manner satisfactory enough to justify its acceptance as an engineering study, in order to obtain the degree for which it has been submitted. This approval does not endorse or approve any statement made, opinion expressed or conclusion drawn therein, but merely approves the thesis for the purpose for which it has been submitted.

Committee of the final examination
for evaluation of the Thesis

_____

_____

_____

_____

** Only in case the thesis is approved.

DECLARATION OF ORIGINALITY AND COMPLIANCE OF ACADEMIC ETHICS

I hereby declare that this thesis contains a literature survey and original research work by the undersigned candidate for the Master of Technology (Nano Science and Technology) program during the academic year 2022-2024.

The information in this document has been gathered and presented according to academic standards and ethical conduct.

I also declare that I have cited and referred to all materials and results that are not original to this work as required by these rules and conduct.

Name: **KOUSTAV SAMADDAR**

Roll Number: **002230701017**

Registration Number: **163817 of 2022-23**

Thesis Title: Study of nitrogen doped reduced graphene oxide (rGO) for its potential application as a Glucose sensor.

SIGNATURE **DATE**

ACKNOWLEDGEMENT

I am grateful to **Dr. Sourav Sarkar, my adviser**, for his consistent encouragement, passion, andwide knowledge throughout my Master's studies and research. He was there for me every step of the way as I worked on my thesis. Your informative comments inspired my entire research project, and I am grateful. In addition, I'd want to express my gratitude to **Prof. Kalyan Kumar Chattopadhyay** and the Thin Film and NanoScience Lab, as well as the Nanoscience and Nanotechnology Lab, for establishing a friendly work environment for me.

Mr. Manas Thakur, my mentor, deserves my gratitude for his direction and assistance with all of my project-related issues, as well as for cooperating with me to make it what it is now.

I gratefully thank **Prof Kalayan Kumar Chattopadhaya, Dr. Sourav Sarkar, Dr. Mahua Ghosh, and Dr. Chandan Kumar Ghosh** for their assistance, support, recommendations, and guidance. They offered a helpful and constructive learning environment, and their excitement inspired me to pursue the research topic with zeal.

Sk Najes Riaz, Dimitra Das, Antika Das, Nabanita Sen, Ratna Sarkar, Suvankar Poddar, Suvra Pal, and Arnab Das, my seniors, deserve my heartfelt gratitude for making my project such a memorable experience. I truly thank Arnab Kmar Saha, Sourav Ghosh, Gourav Payra and my classmates for their assistance and support throughout this course. I could not have completed my project without their assistance. In light of their tremendous aid, my words of gratitude are insufficient.

Finally, I want to express my heartfelt gratitude to my parents and all of my supporters for their love and support.

Abstract

This work describes synthesizing porous nitrogen-doped reduced graphene oxide (N-rGO) via hydrothermal synthesis and it's application as non- enzymatic glucose sensor . Before that, graphene oxide (GO) was prepared using a modified version of Hummer's process. The crystallinity and phase have been verified with an XRD device. Morphological analysis using FESEM images confirms the porous nature. Conversely, comparisons of their UV-vis have been done to help determine the band gaps between GO and rGO. In this project, electrical (resistive) biosensor for glucose monitoring has been experienced. A comparison study of different layers, enzymatic interaction and their out has been carried for the rGO based devices. Here, alpha-glucose has been tested with the biosensor. After a layer-dependent experiment, it can be expressed from the I-V analysis 1layer rGO device has shown a better response than GOx+rGO-coated all devices.1L rGO-coated device also gives better response than 1L GOx+rGO and from LOD curve it can be clearly stated that 1 layer rGO coated device has better sensibility in all aspect.

Table of Contents

- **Chapter 1: Introduction**
  - Introduction
  - Reduced Graphene Oxide
  - Properties of Reduced Graphene Oxide
  - Biosensors and its Applications Introduction:

Types of biosensors Biosensors

- The DNA biosensors
- Magnetic biosensors:
- Thermal biosensors or calorimetric biosensors:
- Piezoelectric biosensors:
- **Optical biosensors:**

Application of Biosensor

- In fermentation processes
- Biosensing technology for sustainable food safety
- In medical field
- Fluorescent biosensors
- Biodefense biosensing applications
- In metabolic engineering
- **Chapter 2: Instrumentation**

- **Characterization techniques**

    Morphological Characterizations

    - Scanning Electron Microscope (SEM)
        - Sample preparation of FESEM
        - Components of FESEM
        - Components of HRTEM

    Phase or Crystallographic characterization

    X-Ray Diffraction (XRD)

    Spectroscopic Characterization

    - UV-vis near infrared spectroscopy
    - Fourier Transform Infrared Spectroscopy (FT-IR)
    - I-V Characterization

- **Chapter 3: Different Synthesis Techniques**
    - GO Synthesis Techniques

        Staudenmaier's (ST) method

        Hummer's method

        Hydrothermal process

        - Advantage of Hydrothermal process
        - Disadvantage of Hydrothermal process
    - Reduction of GO to rGO
    - Metal assisted Chemical etching method
        - Deposition of noble metal
        - Reactions
        - The overall etching process.
    - Catalyst assisted VLS growth process

        Vapor-Liquid-Solid (VLS) mechanism

        Fundamentals of homogeneous nucleation and growth

- **Chapter 4: Literature Review**

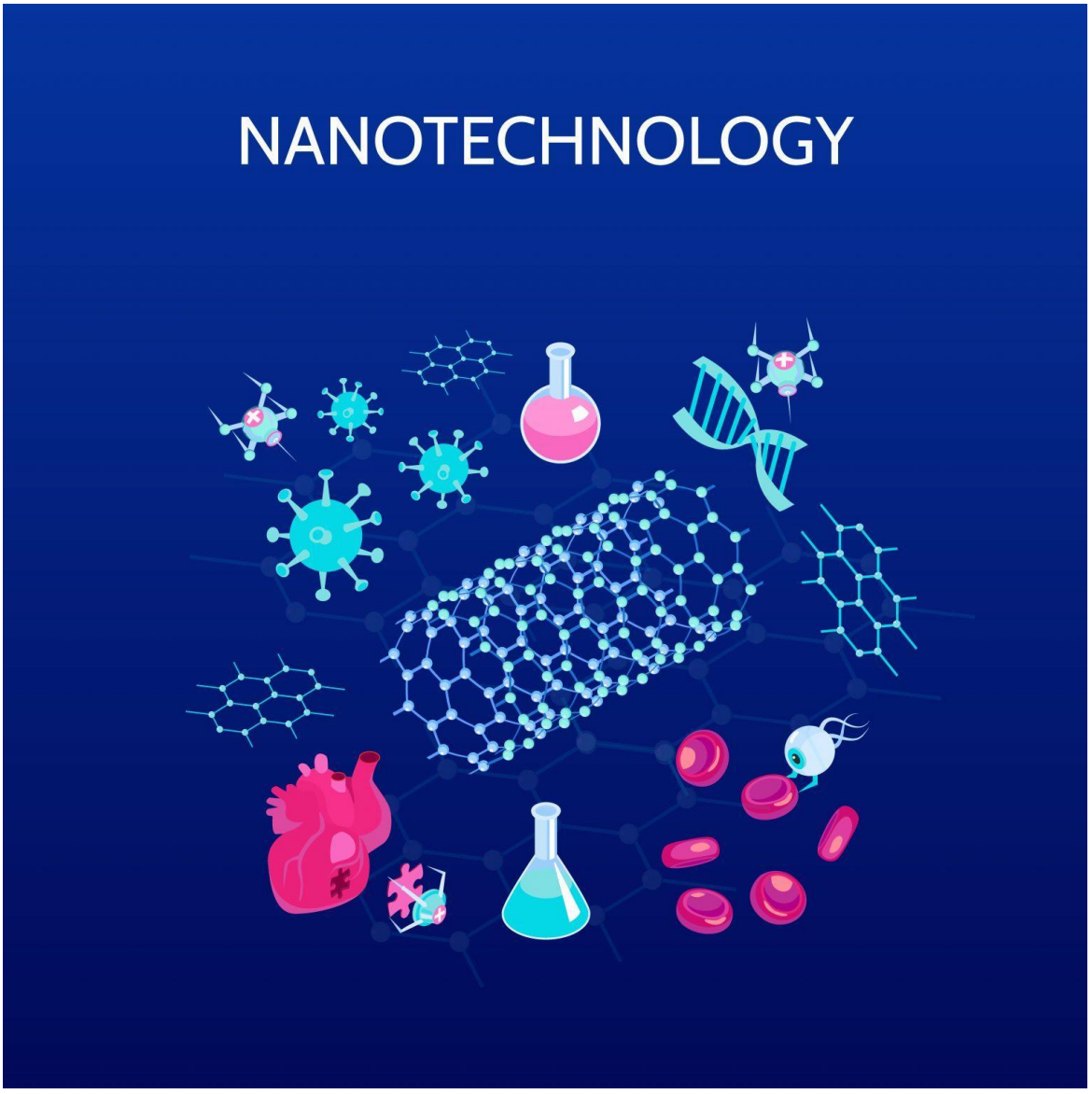
- **Chapter 5: Experiments: Synthesis of samples**
    - Synthesis of Graphene Oxide using modified Hummer's method
        - Materials
        - Sample preparation
    - Synthesis of N-doped reduced Graphene Oxide using Hydrothermal method

- **Chapter 6: Device Fabrication: Part-I (Supercapacitors)**
    - Preparation of FTO based Biosensor
    - Preparation of Multiple layer of Rgo based Biosensor:
    - Preparation of Multiple layer of rGO_Gox based Biosensor
- **Chapter 7: Results and discussions**
    - Morphological Characterizations & analysis
        - Field Emission Scanning Electron Microscopy (FESEM) of N-doped rGO
    - Crystallographic characterization & analysis
        - X-Ray Diffraction (XRD) analysis
    - Spectroscopic Characterization & analysis
        - UV-vis Spectroscopic analysis
        - Fourier Transform Infrared Spectroscopy of NrGO
- **Chapter 8: Device Performance (Biosensor)**
    - IV ch**aracterestics & RV characteristics**
        - **Details of three electrode setup**
        -

Chapter 9: Conclusion:

Chapter-1

Introduction



Introduction:

Our bodies needs Glucose7 (reasonable simple sugar) and that we cannot exist with 0 glucose particularly for Athletes, Faculty Players. The primary energy source for all of our cells, including the brain and muscles. Glucose is six carbon one object ($C_6H_{12}O_6$)-- meaning it has 6 carbons, 12 hydrogens and only six oxygens. As a cyclic molecule, it can cyclize to form glucopyranose. The ability to monitor and control the concentrations of glucose in bodily fluids, such as blood, urine or saliva is essential for good health & optimum performance. For athletes and college sportsmen in particular, this is key because training as well as gaming requires a steady stream of the bodies to deliver energy.

Real-time glucose levels allow athletes to optimize their nutritional intake and timing, which will assist in improving recovery from injury as well as aid peak performance. One example is in the case of intense exercise, which oxidatively burns glucose. An athlete's performance can make it or break by this. Therefore, if we can know its level at a particular time this awareness could be quite powerful. This will allow everyone, but especially athletes using continuous glucose monitoring to have a real time measure of their optimal diet and exercise load for the day. Those with higher average blood glucose have increased risk of stroke, dementia, renal and nerve failure as well - >diagront to be rewritten!! Therefore, the importance of studying and advancing mechanisms for glucose detection in sports health is very high. There are numerous methods where the levels of glucose in biological fluids can be detected. These are the finger prick test, continuous glucose monitoring (CGM), flash monitor and oral glucose tolerance tests. Although these techniques of blood glucose measurement are efficient, they possess some limitations, too. For one thing, there may be a few techniques that seem less likely since they are invasive and could potentially offer some discomfort for the user to have their blood work done. Others perhaps will not provide real time monitoring, a necessity for diseases like diabetes (59).

Furthermore, also spectroscopy (NIR), mid-infrared ((MIR)) Raman and high performance liquid chromatography ((HPLC)) have viability ever since been investigated for glucose detection [465], as well gas/gasless sensor arrays can be implemented for the simultaneous analysis of e.g. glucokinase activity was further quantized by an enzyme-linked immunosorbent assay which is a lateral flow electrochemical sensors technique that detect either superoxide or nitric oxide during enzymatic processes in media culture []. Electrochemical sensors are one possible approach to address these challenges. They function by converting a chemical reaction into an electrical signal that may be read and are often used due to their high sensitivity and specificity. Nanostructures have revolutionized the world of sensors These nanostructures hence make the sensor more sensitive, faster and also improve its selectivity. They also significantly improve the surface area for reactions to occur and this improves both sensitivity as well as response time of the sensor.

Looking at things like wearable glucose sensors, the research is extremely encouraging. This is a completely practical and convenient option for users in contrast to traditional blood sugar monitor sensors as it can measure glucose levels from perspiration or interstitial fluid without the need of a drop of blood. Offering a range of uses for the medical and sports communities, these sensors enable constant monitoring of blood glucose levels that are crucial when it comes to managing energy levels and performance. In that context researching and developing these sensors becomes most critical.

Here, a non-invasive glucose detection system was designed based on the electrochemical sensor GOx/PdO-rGO/C-PE prepared by screen-printing of reduced graphene oxide (rGO) detected in PdO nanoparticles immobilized for cellulose-based substrates. GOx/PdO-rGo/C-PE is a composite material assembly composed of several individual components each contributing unique properties beneficial to the performance of the sensor. GOx is an enzyme which catalyzes the conversion of glucose to D-glucono-δ-lactone and hydrogen peroxide. Due to its fast acting mode of action, excellent stability and specificity it is often called the ideal enzyme. It provides the metabolic response needed for sensing glucose in the sensor. It is known to be a catalytically very active PdO nanoparticle. That in turn can increase the performance of the sensor to higher selectivity and sensitivity towards glucose detection. One

product of chemical reduction is Reduced graphene oxide (rGO). There lie excellent electrical conductivity, high aspect ratio and good biocompatibility in it. On account of this rGO can be an unprecedented material to improve the performance of sensors in sensitivity and speed. Plant materials contain a major amount of cellulose and this compound is the most abundant polysaccharide on Earth. The bio-inspired material provides the sensor a biocompatible and environmentally-friendly substrate. This is because it has a porous structure that allows the other components to be immobilized properly, thereby assisting glucose detection.

Thus, the GOx/PdO-rGO/C-PE sensor using these materials can contribute to non-invasive glucose monitoring valuable in treating diseases such as diabetes (Scheme 1). The glucose detection mechanism has been established on the basis of a series biochemical reaction cascade viz., GOx to induce catalytic activity, PdO NPs for more and continuous development oxygen reduction Owings onto its surface as well rGO with large aspect ratio possessing excellent conductivity are discussed. Thus they are a very promising tool in the fields of biomedical engineering and medicine.

The field of non-invasive glucose monitoring has seen major developments thanks to the advances discussed herein. This sensing electrode construction of the GOx/PdO-rGO/C-PE sensor implies that biochemistry with nanotechnology and materials science shall be integrated making disposable glucose sensors dependable. The sensor performance has been enhanced by employing GOx, PdO nanoparticles-rGO, and a cellulose substrate. It opens new horizons not only for biomedical engineering and medicine, but also for diabetes regulation in humans. The technology has numerous potential applications, including improving athletic performance or providing better patient care in various specialties. As we continue to learn more about these materials and how they work, additional glucose tracking solutions will probably be ever further progressed and stronger in the future.

Reduced Graphene Oxide:

Reduced Graphene oxide is part of the 2D materials family and a hot topic of nanoscience and technology because of its unique properties and efficient applications in various fields of our daily life. Since of its high conductivity and large surface area, single layer graphene is the carbonous substance that researchers are most interested in studying because it may be used to create any type of sensing device. Graphite restacks easily, making the chemical production of large-scale single-layer graphene sheets from raw graphite extremely difficult. To address this issue, graphite sheets are first chemically oxidized to create layered graphene oxide (GO), which is then reduced to create reduced graphene oxide (rGO), which has nearly identical properties to graphene but a larger surface area due to its porous structure. To date, different

reducing agents have been employed to create rGO from GO, including hydrazine, hydroxylamine, urea, dimethyl ketoxime, pyrrole, ammonia, and pyrrolidine. In addition, several oxygen-containing groups have been added, including ascorbic acid, gallic acid, hydroquinone, and metal particles like Fe powder and Zn/HCL. In particular, groups that contain oxygen and nitrogen have been chosen above other chemicals for reduction purposes because these functionalities on the carbon moiety can start the production of sp3 carbon and defect density, which ostensibly opens the door for various electrochemical features. By adjusting the reaction's temperature and duration, optimized rGO with the best electrochemical properties and surface area can be produced. Although forming doped (nitrogen, oxygen, sulfur, etc.) and undoped or pure rGO in room temperature hydrothermally, which implies a 4-electron transfer pathway, is possible utilizing non-toxic biological as a reducing agent, it is of great interest. The appropriate reduction of GO to rGO is thought to induce porosity in the rGO that increases the material's surface area. Good surface area results in a material's good and effective super-capacitive nature.

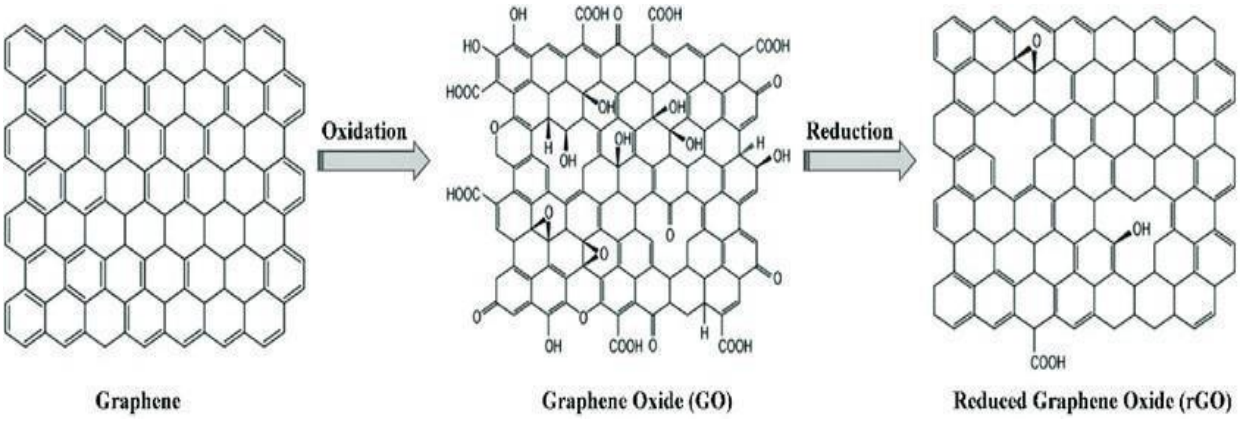


Fig 1.1. Reduction of Graphene oxide into reduced graphene oxide using oxidation (collectedfrom web page)

Properties of Reduced Graphene Oxide(rGO):

Reduced graphene oxide or rGO has lots of interesting properties that are not available in case of 3D materials or bulk materials. This type of 2D material has a layered structure, porous nature and great specific surface area. Due to these reasons, it offers various tunable properties which can be used for various types of applications such as supercapacitors (energy storage system), photodetectors, bio-sensors, temperature sensors etc.

usually have high conductive nature and stability but having less energy density. Thus, these types of materials are not in that much industrial use compared to metal oxides/hydroxides and conducting polymers in terms of supercapacitance. Significantly, due to different defect states, functionalized groups and different dopants such as nitrogen, oxygen, boron etc., reduced graphene oxide overcomes most of its difficulties in order to become a good supercapacitor and photodetector materials. Due to well-engineered pores and great surface area of rGO, it is easy to get more contact with electrolytes which facilitates easier diffusion of ions throughout the system.

The porous nature and different defect states of the reduced graphene oxide layer brings an indirect band gap of lower range which causes easier transportation of electrons through the bands (conduction band and valence band). Thus, it has a low work function which leads to a great photo-electric effect. Due to this it has a wide range of opto-electronic applications, such as photodetector, photodiode etc. The band gap of pure rGO can be tuned using different dopants which will cause multiple applications in different fields.

Biosensors and its Applications Introduction:

What is a Biosensor?

The most widely accepted definition of a biosensor is: “an analytical device which incorporates a biologically active element with an appropriate physical transducer to generate a measurable signal proportional to the concentration of chemical species in any type of sample”.

Type of Biosensors:

Biosensors can be categorized according to the basic principles of signal transduction and biorecognition elements. In the general scheme of a biosensor

the bio bio-recognition element responds to the target compound and the transducer converts the biological response to a detectable signal, which can be measured electrochemically, optically, acoustically, mechanically, calorimetrically, or electronically, and then correlated with the analyte concentration. Biological elements include enzymes, antibodies, microorganisms, biological tissue, and organelles. When the binding of the sensing element and the analyte is the detected event, the instrument is described as an affinity sensor. When the interaction between the biological element and the analyte is accompanied or followed by a chemical change in which the concentration of one of the substrates or products is measured the instrument is described as a metabolism sensor.

Finally, when the signal is produced after binding the analyte without chemically changing it but by converting an auxiliary substrate, the biosensor is called a catalytic sensor. The method of transduction depends on the type of physicochemical change resulting from the sensing event. Often, an important ancillary part of a biosensor is a membrane that covers the biological sensing element and has the main functions of selective permeation and diffusion control of analyte, protection against mechanical stresses, and support for the biological element.

Types of biosensors Biosensors

started in the 1960s by the pioneers Clark and Lyons. Various types of biosensors being used are enzyme-based, tissue based, immunosensors, DNA biosensors, and thermal and piezoelectric biosensors. The first enzyme-based sensor was reported by Updike and Hicks in 1967. Enzyme biosensors have been devised on immobilization methods, i.e. adsorption of enzymes by van der Waals forces, ionic bonding or covalent bonding. The commonly used enzymes for this purpose are oxidoreductases, polyphenol oxidases, peroxidases, and amino oxidases. The first microbe-based or cell-based sensor was actualized by Diviès. The tissues for tissue-based sensors arise from plant and animal sources. The analyte of interest can be an inhibitor or a substrate of these processes. Rechnitz9 developed the first tissue based sensor for the determination of amino acid arginine. Organelle-based sensors were made using membranes, chloroplasts, mitochondria, and microsomes . However, for this type of biosensor, the stability was high, but the detection time was longer, and the specificity was reduced.

The DNA biosensors

were devised on the property that a single-strand nucleic acid molecule is able to recognize and bind to its complementary strand in a sample. The interaction is due to the formation of stable hydrogen bonds between the two nucleic acid strands.

Magnetic biosensors:

miniaturized biosensors detecting magnetic micro- and nanoparticles in microfluidic channels using the magnetoresistance effect have great potential in terms of sensitivity and size**.**

Thermal biosensors or calorimetric biosensors:

are developed by assimilating biosensor materials as mentioned before into a physical transducer.

Piezoelectric biosensors:

are of two types: the quartz crystal microbalance and the surface acoustic wave device. They are based on the measurement of changes in resonance frequency of a piezoelectric crystal due to mass changes on the crystal structure.

Optical biosensors:

consist of a light source, as well as numerous optical components to generate a light beam with specific characteristics and to beeline this light to a modulating agent, a modified sensing head along with a photodetector.

Applications of biosensors:

Some examples of the fields that use biosensor technology include: General healthcare

Monitoring

 Screening for disease

 Clinical analysis and diagnosis of disease

 Veterinary and agricultural applications

 Industrial processing and monitoring

 Environmental pollution control

Biosensors have been applied in many fields namely food industry, medical field, marine sector etc., and they provide better stability and sensitivity as compared with the traditional methods. In food processing, monitoring, food authenticity, quality and safety) Ghasemi-Varnamkhasti et al. worked on the monitoring of aging of beer using enzymatic biosensors, based on cobalt phthalocyanine. These biosensors evinced a good capability to monitor the ageing of beer during storage. Biosensors are used for the detection of pathogens in food. Presence of

Escherichia coli in vegetables, is a bioindicator of fecal contamination in food. E. coli has been measured by detecting variation in pH caused by ammonia (produced by urease–E. coli antibody conjugate) using potentiometric alternating biosensing systems. Washing the vegetables such as sliced carrots and lettuce with peptone water provides us with the liquid phase. It is then separated by amalgamating it in a sonicator, to disaffiliate bacterial cells from food items. Enzymatic biosensors are also employed in the dairy industry. A biosensor, based on a screen-printed carbon electrode, was integrated into a flow cell. Enzymes were immobilized on electrodes by engulfment in a photocrosslinkable polymer. The automated flow-based biosensor could quantify the three organophosphate pesticides in milk. One of the popular food additives extensively used today are sweeteners, which are adversely causing undesirable diseases including dental caries, cardiovascular diseases, obesity and type-2 diabetes

In fermentation processes

In fermentation industries, process safety and product quality are crucial. Thus effective monitoring of the fermentation process is imperative to develop, optimize and maintain biological reactors at maximum efficacy. Biosensors can be utilized to monitor the presence of products, biomass, enzymes, antibodies or by-products of the process to indirectly measure the process conditions. Biosensors precisely control the fermentation industry and produce reproducible results due to their simple instrumentation, formidable selectivity, low prices and easy automation. Nowadays, several kinds of commercial biosensors are accessible; capable of detecting biochemical parameters (glucose, lactate, lysine, ethanol etc.) and are widely used in China, occupying about 90% of its market.

Biosensing technology for sustainable food safety

The term food quality refers to the appearance, taste, smell, nutritional value, freshness, flavor, texture and chemicals. Smart monitoring of nutrients and fast screening of biological and chemical contaminants are of paramount importance, when it comes to food quality and safety. Material science, nanotechnology, electromechanical and microfluidic systems are striding in to make sensing technology imminent for use in the market. Efforts are being made for developing control systems ensuring food quality and safety and, as a consequence, human health. Glucose monitoring becomes indispensable as during storage the food content and composition may get altered.

In medical field

In the discipline of medical science, the applications of biosensors are growing rapidly. Glucose biosensors are widely used in clinical applications for diagnosis of diabetes mellitus, which requires precise control over blood-glucose levels. Blood-glucose biosensors usage at home accounts for 85% of the gigantic world market. Biosensors are being used pervasively in the medical field to diagnose infectious diseases. A promising biosensor technology for urinary tract infection (UTI) diagnosis along with pathogen identification and antimicrobial susceptibility is under study. Fluorescent biosensors Fluorescent biosensors are imaging agents, for use in cancer and drug discovery. They have enabled insights into the role and regulation of enzymes at cellular level. GFP-based and genetically encoded FRET biosensors play a vital role.

Fluorescent biosensors

are used in drug discovery programmes for the identification of drugs by high throughput, high content screening approaches, for post screening analysis of hits and optimization of leads**.**

Biodefense biosensing applications

Biosensors can be used for military purposes at times of biological attacks. The main motive of such biosensors is to sensitively and selectively identify organisms posing threat in virtually real time called biowarfare agents (BWAs) namely, bacteria (vegetative and spores), toxins and viruses. Several attempts to devise such biosensors have been done using molecular techniques which are able to recognize the chemical markers of BWAs. Nucleic acid-based sensing systems are more sensitive than antibody based detection methods as they provide gene-based specificity, without utilizing amplification steps to attain detection sensitivity to the required levels. The human papillomavirus HPV (double stranded DNA virus) has been categorized into two types: HPV 16 and 18; and is related to invasive cervical cancer. HPVs can be rapidly detected using a novel leaky surface acoustic wave peptide nucleic acid biosensor with double twoport resonators. This probe directly detects HPV genomic DNA without polymerase chain reaction amplification, and can also bind to the target DNA sequences with a lot of efficacy and precision**.**

In metabolic engineering

Environmental concerns and lack of sustainability of petroleum-derived products are gradually exhorting need for development of microbial cell factories for synthesis of chemicals. Researchers view metabolic engineering as the enabling technology for a sustainable bioeconomy**.**

Biosensors in plant biology

Revolutionary new technologies in the areas of DNA sequencing and molecular imaging, have lead to advancements in plant science

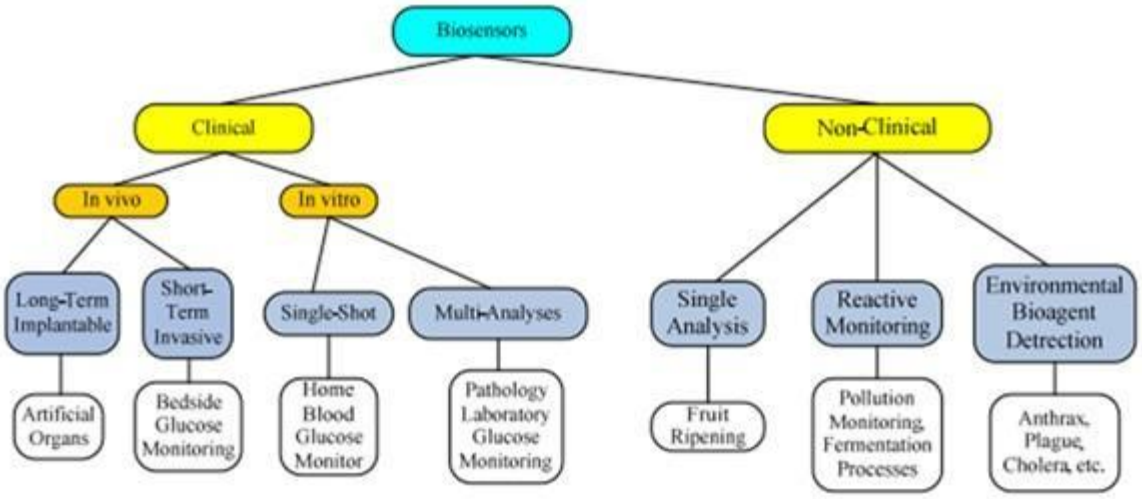


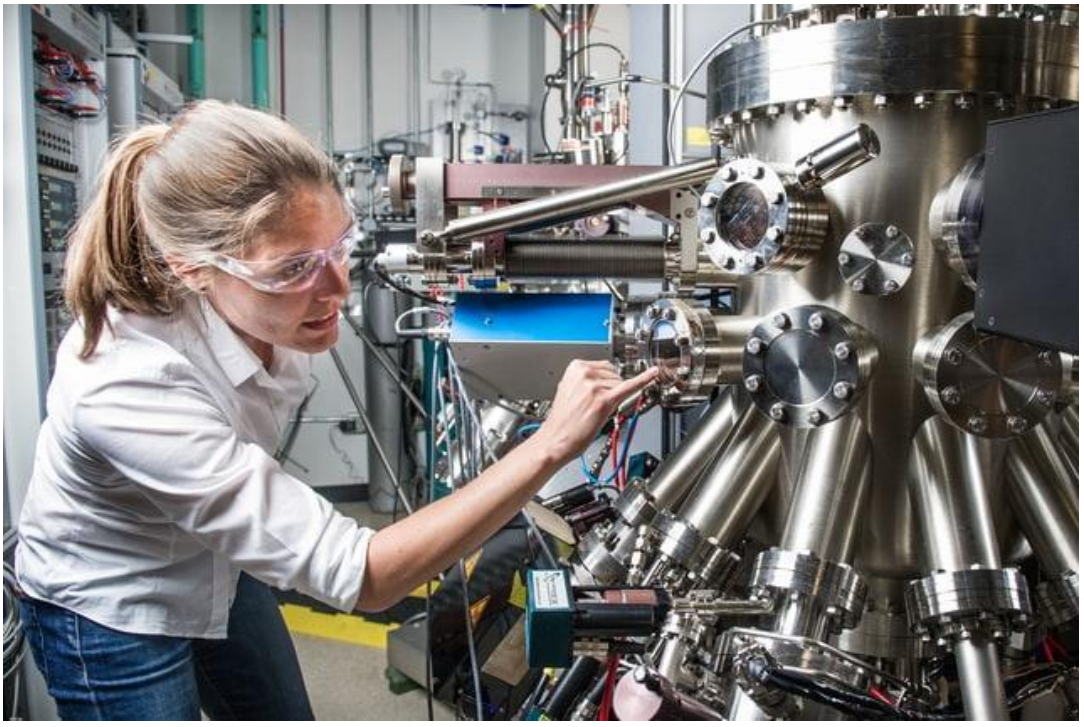
Fig. 2: Potential Applications of Biosensors.

References:

1. S. Priya, D.J. Inman, Energy Harvesting Technologies, 2009, pp. 1e517, https://doi.org/10.1007/978-0-387-76464-1.
2. J.H. Jung, M. Lee, J. Hong, Y. Ding, C. Chen, L. Chou, Z.L. Wang, Lead-free NaNbO3 Nanowires for a High Output Piezoelectric, 2011, pp. 10041e10046, https://doi.org/10.1021/nn2039033
3. Monroy, E.; Calle, F.; Pau, J.L.; Munoz, E.; Omnes, F.; Beaumont, B.; Gibart, P. AlGaN-Based UV Photodetectors. J. Cryst. Growth 2001, 230, 537-543.
4. Brubaker DG, Fuller ML (1945) J Appl Phys 16:128
5. Klingshirn C, Hauschild R, Priller H, Zeller J, Decker M, Kalt H (2006) Adv Spectrosc Lasers Sens 231:277
6. Özgür, Ü.; Alivov, Y.A.; Liu, C.; Teke, A.; Reshchikov, M.A.; Doğan, S.; Avrutin, V.; Cho, S.J.; Morkoç, H. A Comprehensive Review of ZnO Materials and Devices. J. Appl. Phys. 2005, 98, 041301.
7. Look, D.C. Recent Advances in ZnO Materials and Devices. Mater. Sci. Eng. B 2001, 80, 383-387.
8. K. Batra, N. Sinha, S. Goel, H. Yadav, A.J. Joseph, B. Kumar, Enhanced dielectric, ferroelectric and piezoelectric performance of Nd-ZnO nanorods and their application in flexible piezoelectric nanogenerator, J. Alloy. Compd. 767 (2018) 1003e1011, https://doi.org/10.1016/j.jallcom.2018.07.187
9. S. Goel, N. Sinha, H. Yadav, S. Godara, A.J. Joseph, B. Kumar, Ferroelectric Gddoped ZnO nanostructures: enhanced dielectric, ferroelectric and piezoelectric properties, Mater. Chem. Phys. 202 (2017) 56e64, https://doi.org/10.1016/j.matchemphys.2017.08.067
10. Angshuman Deka and Karuna Kar Nanda, A comparison of ZnO films deposited on indium tin oxide and soda lime glass under identical conditions, AIP ADVANCES 3, 062104 (2013), http://dx.doi.org/10.1063/1.4811091.
11. D. Nunes, A. Pimentel, A. Gonçalves, S. Pereira, R. Branquinho, P. Barquinha, E Fortunato and R Martins, Metal oxide nanostructures for sensor applications, Semiconductor Science and Technology 34[4] 043001 (2019), https://doi.org/10.1088/1361-6641/ab011e
12. Jayanta Kumar Behera.Synthesis and Characterization of Nano-particles.M.Tech Thesis, NIT Rourkela.

Chapter-2

Instrumentation



Characterization Techniques:

There are several different methods to characterize the sample to determine its phase, morphology, band gap, lattice vibration, crystallite size, interplanar distance, crystal plane etc. Here, in this work also these methods and machineries are being used to determine various properties of the prepared samples. There are mainly 3 types of characterization analysis that one sample can have, i.e.,

- **Phase or crystallographic characterization**
- **Spectroscopic characterization.**

These three types of characterization techniques include a wide range of different apparatus and machineries. In this chapter major instruments and their basic working principle which were used in this project will be discussed briefly.

➢ Morphological Characterization:

Morphological characterization defines as the technique or method to get information about th

e morphology of the sample in micro and nano level. In nanotechnology, ordinary optical microscopes can not be used due to their limited focus range which is not able to get the information at the nano level. Hence, the need for electron microscopes has emerged resulting in two types of very important electron microscopes, i.e., **Scanning Electron Microscope (SEM)** and **Transmission Electron Microscope (TEM)**.

- **Scanning Electron Microscope (SEM):**

  One of the most adaptable tools for inspecting and deciphering the morphology of microstructures is the scanning electron microscope (SEM). The surface of the object is routinely scanned by a focused electron beam in a scanning electron microscope (SEM), yielding a significant number of signals. An image is produced from these electron impulses and displayed on a cathode ray tube (CRT). There are two techniques to produce the electron beam:

  a) Thermionic emission; b) Field emission.

  Thermal energy is used to regulate the source's electron emission to produce thermionic emission. In modern electron microscopes, field emission electron guns (FEG) are a

great replacement for thermionic electron guns. Very minute topographic characteristics on the surface of whole or fragmented objects can be observed with a FESEM. Researchers in the fields of biology, chemistry, and physics utilize this technique to examine structures as small as 1 nanometer, or billionths of a millimeter. Organelles and DNA material in cells, synthetic polymers, and microchip coatings can all be studied with the FESEM.

b) **Sample preparation for FESEM:**

The specimens that can be analyzed must be compatible with high vacuum (10-5 mbar), as the SEM is operated under high vacuum. This suggests that liquids and objects made of volatile substances, like water, cannot be directly studied. To prevent contaminating the SEM specimen chamber, fine powder samples must also be firmly connected to a specimen holder substrate. A thin conductive layer must be sprayed or evaporated onto non-conductive materials before they are attached to a conductive specimen container. Common coating materials include carbon, Au, Pt, Pd, and their alloys.

c) **Components of FESEM:**

- **Electron Guns:**

Modern FESEM systems require a constant electron beam from the electron cannon that has a high current, a small spot size, configurable energy, and minimal energy dispersion. A variety of electron guns are used in a FESEM system, and the quality of the electron beam produced by each differs greatly. The tungsten "hairpin" or lanthanum hexaboride (LaB6) cathodes used in the first FESEM systems have since been replaced by field emission sources, which provide more current and less energy dispersion. The longevity of the emitter is a crucial consideration when selecting electron sources.

- **Electron Lenses:**

Electron beams can be concentrated by electrostatic or magnetic fields. The FESEM system, however, solely employs a magnetic field since an electron beam governed by one has less aberration. Electromagnets can be used to alter the electrons' routes.

- **Condenser Lenses:**

The electron beam will diverge after passing through an anode plate from the emission source. The electron beam is brought together and collimated by the condenser lens into a nearly parallel stream. Two rotationally symmetric iron pole pieces form a magnetic lens, and a copper winding generates the magnetic field. The center of each pole piece has a hole through which the electron beam can travel. Through a lens-gap between the two pole components, the magnetic field shapes (focuses) the electron beam. Condenser lens current can be changed to change the focus point's location.

- **Scan Coils:**

The scan coils cause the electron beam to be zigzagged as it passes over the object. The development of the image on the display and the scan movement are coordinated. The scan velocity controls both the screen's refresh rate and the amount of noise in the image. In scan coils, upper and lower coils are frequently utilized to avoid the formation of a circular shadow at low magnification.

- **Objective Lens:**

The electron beam will diverge below the condenser aperture. The electron beam is de-magnified further and focused into a probe point on the specimen surface using objective lenses. The diameter of the electron beam on the specimen surface (spot size), which affects image resolution, decreases as aperture size and fundamentals of Scanning Electron Microscopy increase.

- **Stigmator Coil:**

The stigmator coils are used to rectify inconsistencies in the beam's x and y deflection, resulting in a perfectly round beam. When the beam is ellipsoidal rather than circular, the picture seems fuzzy and stretched.

Thermal energy is used to regulate the source's electron emission to produce thermionic emission. In modern electron microscopes, field emission electron guns (FEG) are a great replacement for thermionic electron guns. Very minute topographic characteristics on the surface of whole or fragmented objects can be observed with a FESEM. Researchers in the fields of biology, chemistry, and physics utilize this technique to examine structures as small as 1 nanometer, or billionths of a millimeter. Organelles and DNA material in cells, synthetic polymers, and microchip coatings can all be studied with the FESEM.

- **Sample preparation for FESEM:**

The specimens that can be analyzed must be compatible with high vacuum (10-5 mbar), as the SEM is operated under high vacuum. This suggests that liquids and objects made of volatile substances, like water, cannot be directly studied. To prevent contaminating the SEM specimen chamber, fine powder samples must also be firmly connected to a specimen holder substrate. A thin conductive layer must be sprayed or evaporated onto non-conductive materials before they are attached to a conductive specimen container. Common coating materials include carbon, Au, Pt, Pd, and their alloys.

evaporated onto non-conductive materials before they are attached to a conductive specimen container. Common coating materials include carbon, Au, Pt, Pd, and their alloys.

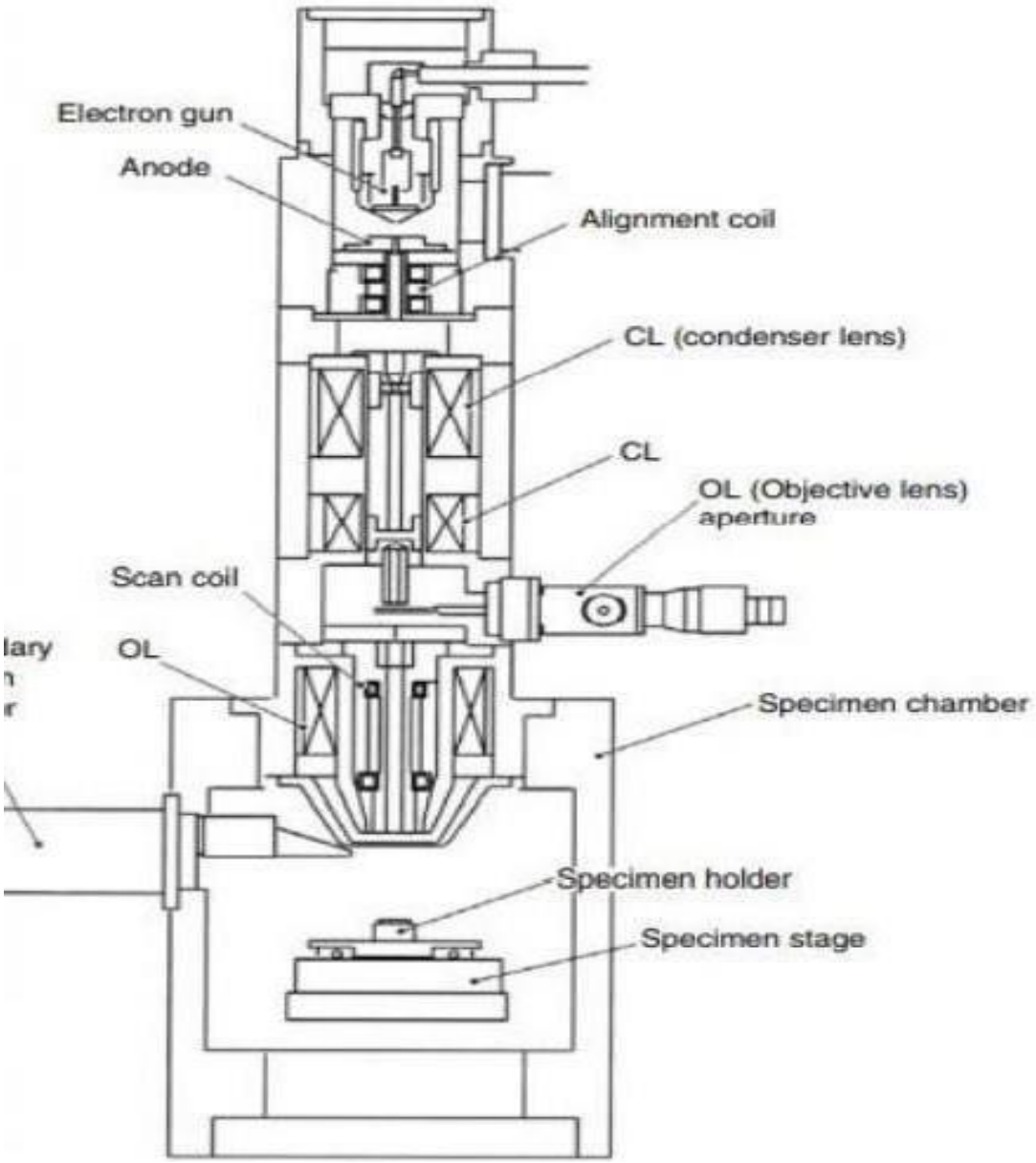


Fig 2.1. Schematic diagram of FESEM

- **Object Chamber:**

The object is coated with a conductive coating before being set on a particular holder. The object is anchored on a moveable stage and introduced into the high vacuum section of the microscope through an exchange chamber. The secondary electron emission detector (scintillator) is placed behind the object holder in the chamber.

- **Image Information:**
  Complex interactions take place when an electron beam impinges on a specimen surface in a FESEM and stimulates various signals for FESEM inspection. It is possible to collect and display secondary electrons, back scattered electrons (BSEs),



Fig 2.2. FESEM (Hitachi S-4800) set up

transmitted electrons, and specimen current on a monitor. To determine the specimen's composition, the excited x-ray or Auger electrons are analysed. This part will cover the interactions of the electron beam with the specimen surface as well as the idea behind making pictures out of different signals.

- **X-Ray Diffraction (XRD):**

X-rays are a form of electromagnetic radiation that has high energies and short wavelengths on the order of the atomic spacing for solids. When a beam of x-rays impinges on a solid material, a portion of this beam will be scattered in all directions by the electron associated with each atom or ion that lies within the beam's pathway.

Let us now examine the necessary conditions for diffraction of X-rays by a periodic arrangement of atoms. Diffraction occurs when a wave encounters a series of regularly spaced obstacles that are capable of scattering the wave and have spacing that are comparable in magnitude to the wavelength. Furthermore, diffraction is a consequence of specific phase relationships established between two or more waves that have been scattered by the obstacles. The phase relationship between the scattered waves, which will depend upon the difference in path length is important. One possibly results when its pathway length is an integral number of wavelengths.

Bragg's Law:

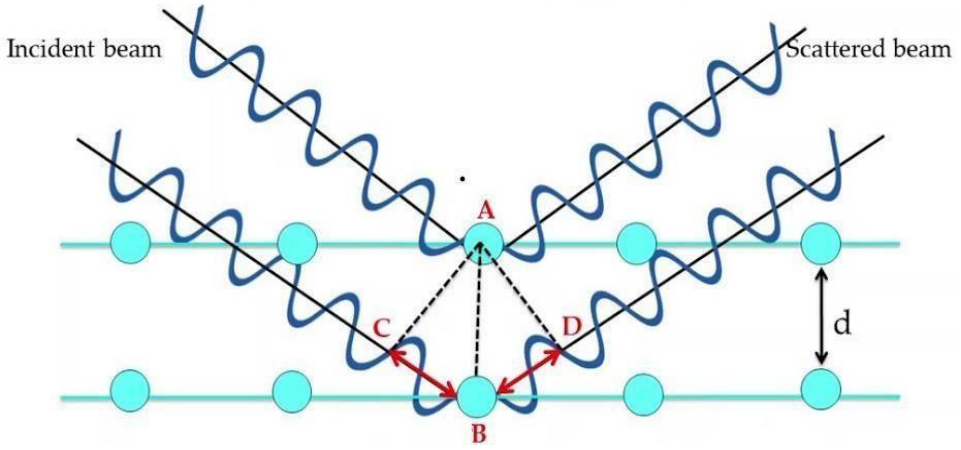


Fig 2.3. Brag's Law of diffraction

Considering the two parallel planes of atoms, which have the same h, k and l Miller indices and are separated by the interplanar spacing d. Now assuming a parallel, monochromatic and coherent (in-phase) beam of x-rays of wavelength λ is incident on these two planes at an angle of Θ. Two rays in this beam are scattered by atoms A and B. Constructive interference of the scattered waves occur also an angle of Θ to the planes, if the path length difference (i.e. CB+BD) between these waves is equal to a whole number, n, of wavelengths. So, the condition for diffraction is

$n\lambda = CB + BD$

or, $n\lambda = d\sin\Theta + d\sin\Theta$

or, $n\lambda = 2d\sin\Theta$



Fig 2.5. X-Ray Diffraction (Bruker D8 advance)

Particle Size determination by Scherrer's formula:

Experimentally obtained diffraction patterns of the sample are compared with the standard powder diffraction files published by the JCPDS. The average grain size of the samples was calculated using Scherrer's formula:

$$D = \frac{0.9\lambda}{\beta \cos \theta}$$

Where, λ is the wavelength of x-rays,

And β is the full width at half maximum intensity in radians.

It is important to realize that the Scherrer's formula provides a lower bound on the particle size. The reason behind this is that a variety of factors can contribute to the width of a diffraction peak; besides particle size, the most important of these are actually dependent on the factors like inhomogeneous strain and instrumental errors. If all of these other factors contributing to the peak width were zero, then the peak width would be determined solely by the particle size and the Scherrer's formula would apply. If the other contributors to the peak width is non-zero, then the particle size can be larger than predicted by this formula, with the "extra" peak width coming from the other facts.

➢ Spectroscopic characterization:

- **UV-VIS near infrared Spectroscopy:**

The optical transmittance, absorbance, and reflectance in the ultraviolet-visible spectral area are measured using UV-Vis-NIR Spectrophotometers. Measurements of optical transmittance, absorbance, and reflectance in the ultraviolet visible spectral area are made using UV-Vis near Infrared (UV- Vis-NIR) Spectrophotometers. The amount of radiation that is absorbed, transmitted, or reflected at each wavelength is quantified using UV-Vis absorption spectroscopy. Typically, this is done by measuring the absorption while scanning the wavelength range. To determine the degree of multiple bond or aromatic conjugation within molecules, it is frequently employed in organic chemistry. The method can be expanded to include gasses and solids as well as go beyond absorption to measure reflected light as opposed to transmitted light.

Light absorption can be described by two fundamental laws as:

- **Lambert's Law:**

The proportion of incident light absorbed by a transparent medium is independent of the intensity of the light (provided that there is no other physical or chemical change to the medium). Therefore, successive layers of equal thickness will transmit an equal proportion of the incident energy.

Lambert's law can be expressed by

$$\frac{I}{I_0} = T$$

Where I is defined as the intensity of transmitted light, I_0 is defined as intensity of incident light and T is the transmittance.

- **Beer's Law:**

  The absorption of light is directly proportional to both the concentration of the absorbing medium and the thickness of the medium in the light path.

  A combination of the two laws (known jointly as the Beer-Lambert Law) defines the relationship between absorbance (A) and transmittance (T).

$$A = log\frac{I_0}{I} = log\frac{100}{T} = \varepsilon cb$$

Where, A is absorbance, ε is molar absorptivity, c is molar concentration and b is path length.

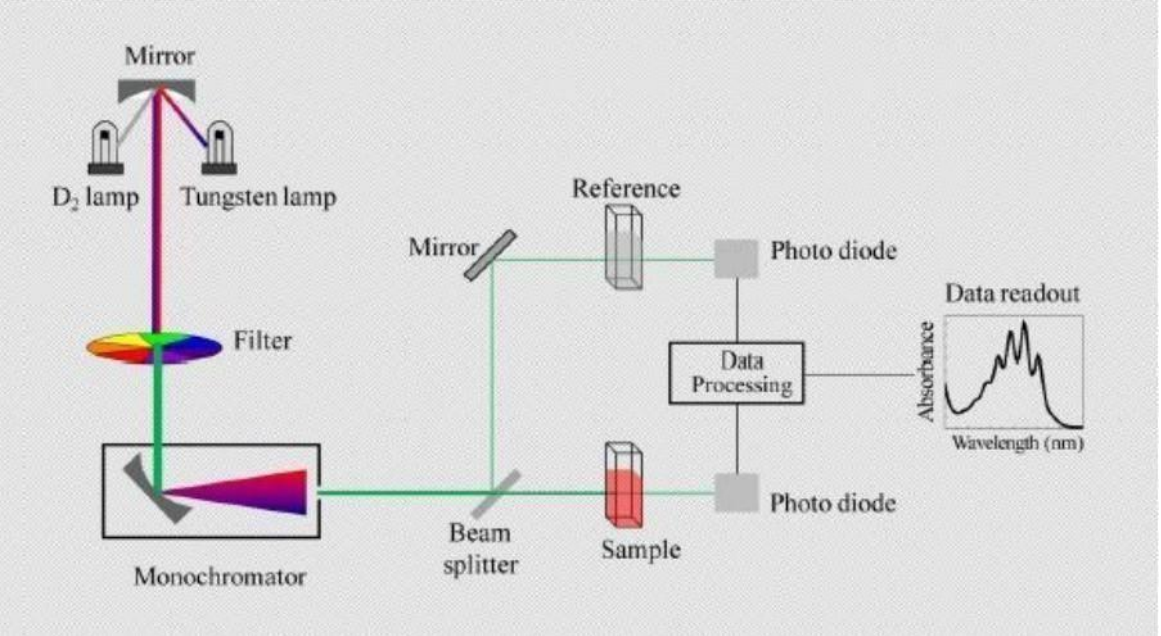


Fig 2.6. Basic working principle of UV-Vis spectroscopy

- **LIGHT REFLECTION AND REFLECTANCE SPECTRA:**

The spectrometer beam is directed into the sample, where it is reflected, dispersed, and transmitted through the sample material, resulting in diffuse reflectance (shown on the right). The accessory collects the back reflected, diffusely dispersed light (part of which is absorbed by the sample) and directs it to the detector optics. Diffuse reflection refers to the portion of a beam that is dispersed within a sample and returns to the surface.

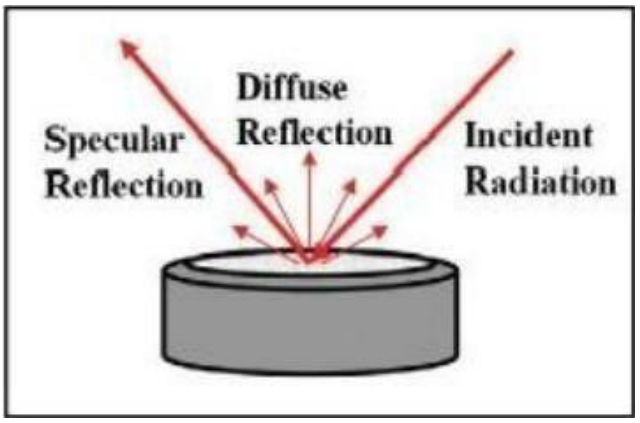


Fig 2.7 Diffuse and Specular Reflectance

Particle size, refractive index, homogeneity, and packing are further parameters that contribute to excellent spectral quality in diffuse reflectance sampling. The raw diffuse reflectance spectra will seem different from its transmission counterpart despite all of these sample preparation techniques (stronger than expected absorption from weak IR bands).

To correct for these discrepancies, a Kubelka-Munk conversion can be performed to a diffuse reflectance spectrum.

Kubelka-Munk Function:

$$F(R) = \frac{(1-R)^2}{R} = \frac{k}{s}$$

R stands for the sampled layer's absolute reflectance, k for the molar absorption coefficient, and s for the scattering coefficient.

This spectral conversion for ibuprofen obtained via diffuse reflectance is illustrated in thespectrum above. The Kubelka-Munk converted spectrum for ibuprofen compares well to the transmission spectrum and is easily recognised using a transmission spectral data library search.

- **Components of UV-Vis:**

i) Spectrophotometer consists of the following components
ii) A source of radiation of appropriate wavelength.
iii) Monochromator and optical geometry.
iv) Filter sample compartment.
v) Detector, photomultiplier, measuring system and computer.

The UV VIS spectra carried out by the Shimadzu UV 3600 spectrophotometer.



Fig .2.8. UV-VIS-NIS (SHIMADZU UV-3600) Spectrophotometer

- **FOURIER TRANSFORM INFRA-RED SPECTROSCOPY (FTIR):**

For studying the vibrational properties of synthesis materials, FTIR spectroscopy is a very useful tool. The band positions and absorption peak of thin films are influenced not only by their chemical composition and structure, but also by their morphology.

The preferred method of infrared spectroscopy is known as Fourier Transform InfraRed (FT-IR). Infrared spectroscopy involves passing IR radiation through a sample. The sample absorbs some of the infrared radiation and passes some of it through (transmitted). The resulting spectrum depicts the sample's molecular absorption and transmission, resulting in a molecular fingerprint. No two unique molecular structures produce the same infrared spectrum, just like a fingerprint. As a result, infrared spectroscopy can be used for a variety of purposes.

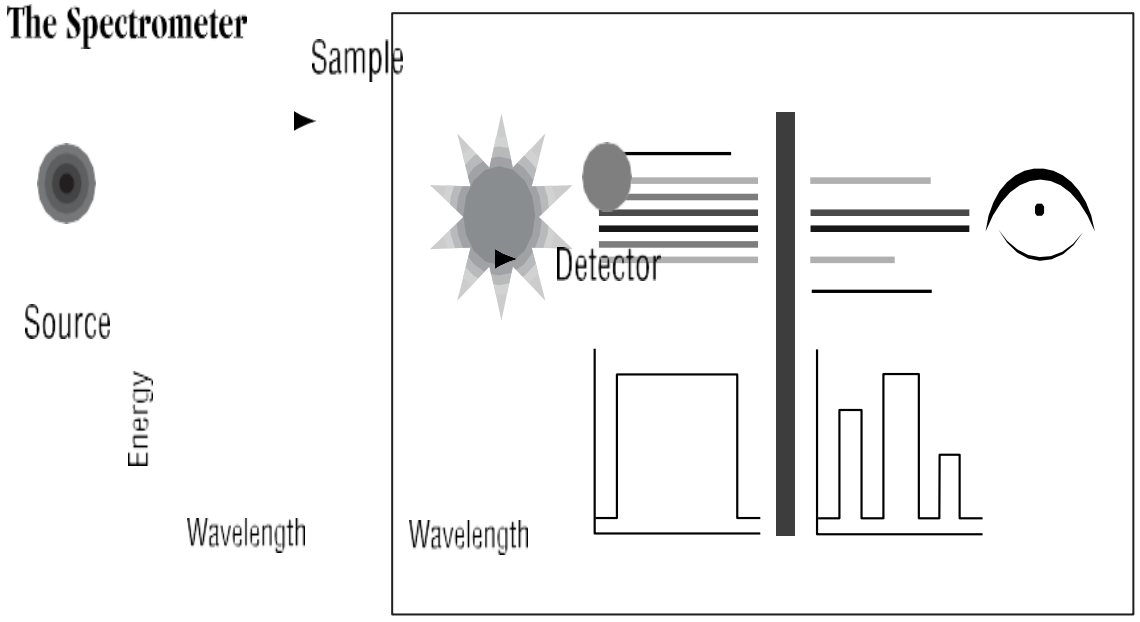


Fig2.9. Spectrometer

So, what kind of information can FT-IR give you?

• It can determine the quality or consistency of a sample

• It can determine the number of components in a mixture

• It can identify unknown materials

WHY INFRARED SPECTROSCOPY?

For over seventy years, infrared spectroscopy has been a workhorse technique in the laboratory for materials analysis. An infrared spectrum is a sample's fingerprint, with absorption peaks corresponding to the frequencies of vibrations between the bonds of the material's atoms. Because each material is made up of a different set of atoms, no two compounds have the same infrared spectrum. As a result, infrared spectroscopy can be used to positively identify (qualitatively analyze) any type of material. Furthermore, the size of the peaks in the spectrum indicates the amount of material present. Infrared is an excellent tool for quantitative analysis thanks to modern software algorithms.

OLDER TECHNOLOGY:

The first infrared instruments were dispersive in nature. Individual frequencies of energy emitted from the infrared source were separated using these instruments. A prism or grating was used to accomplish this. A visible prism separates visible light into its colours, and an infrared prism does the same (frequencies). A grating is a more modern dispersive element that separates infrared energy frequencies better. The detector counts the amount of energy that has passed through the sample at each frequency. As a result, a spectrum is created, which is a plot of intensity against frequency.

For several reasons, Fourier transform infrared spectroscopy is preferred to dispersive or filter methods of infrared spectral analysis:

• It is a non-destructive technique

• It provides a precise measurement method that does not require external calibration

• It can increase speed, collecting a scan every second

• It can increase sensitivity – one second scans can be co-added together to ratio out random noise

• It has greater optical throughput.

Why FT-IR?

In order to overcome the limitations of dispersive instruments, Fourier Transform Infrared (FT-IR) spectrometry was developed. The slow scanning process was the main issue. It was necessary to develop a method for measuring all infrared frequencies simultaneously rather than individually. An interferometer, a very simple optical device, was used to develop a solution. The interferometer generates a unique signal that contains all of the infrared frequencies "encoded." The signal can be measured very quickly, usually in a fraction of a second. As a result, the time element per sample is reduced from several minutes to a few seconds. A beam splitter is used in most interferometers to divide the incoming infrared beam into two optical beams.

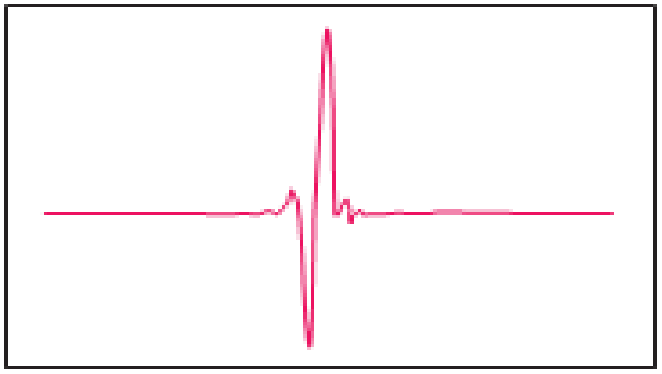


Fig 2.10. An interferogram signal

A flat mirror, which is fixed in place, reflects one beam. The other beam reflects off a flat mirror that moves a very short distance (typically a few millimeters) away from the beam splitter thanks to a mechanism. When the two beams meet again at the beam splitter, they reflect off their respective mirrors and are recombined. The signal that exits the interferometer is the result of these two beams "interfering" with each other because one beam's path is fixed and the other's is constantly changing as its mirror moves.

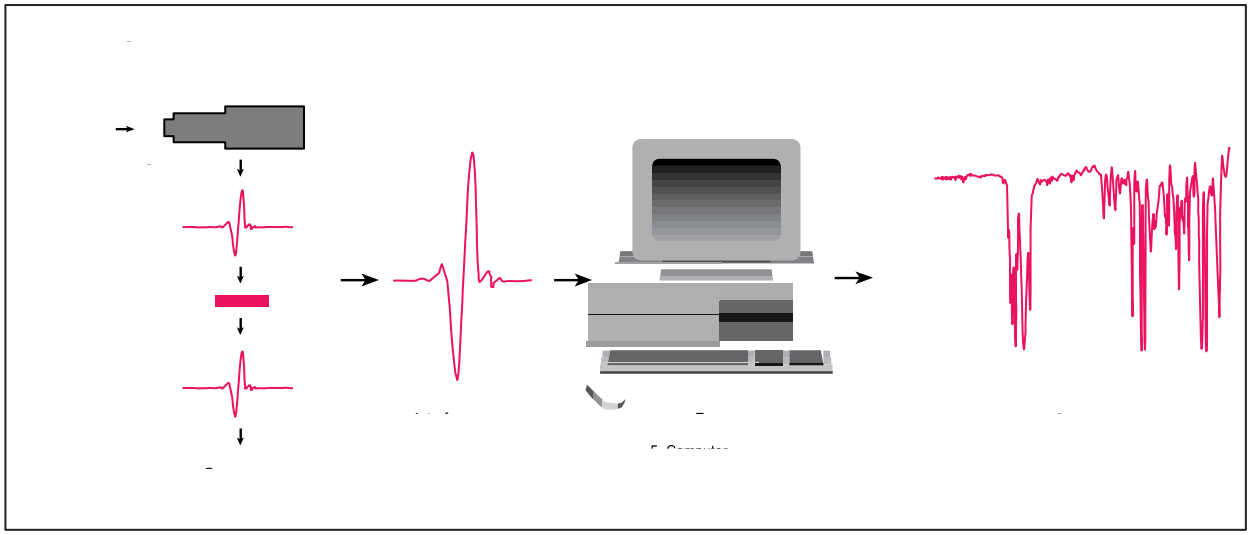


Fig 2.11. Process of generating an FTIR spectra

The resulting signal is known as an interferogram, and it has the unique property of having information about each infrared frequency that comes from the source in every data point (a function of the moving mirror position) that makes up the signal. This means that all frequencies are measured simultaneously as the interferogram is measured. As a result of the interferometer's use, measurements are extremely quick. The measured interferogram signal cannot be interpreted directly because the analyst requires a frequency spectrum (a plot of the intensity at each individual frequency) in order to make an identification. It's necessary to have a way of "decoding" the individual frequencies. The Fourier transformation, a well-known mathematical technique, can be used to accomplish this. The computer performs this transformation and then presents the user with the desired spectral information for analysis.

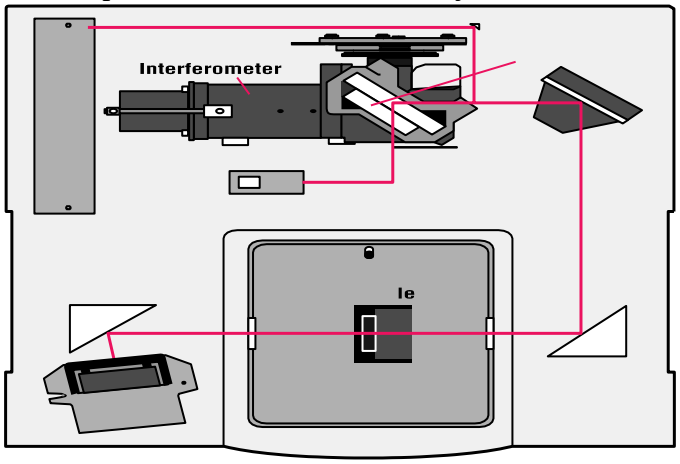


Fig 2.12. A simple spectrometer layout

THE SAMPLE ANALYSIS PROCESS:

The standard instrumental procedure goes like this:

1. **The Source**: A glowing black-body source emits infrared energy. This beam passes through an aperture that regulates how much energy is delivered to the sample (and, ultimately, to the detector).

2. **The Interferometer**: The beam passes through the interferometer, which performs "spectral encoding." The interferogram signal is then output from the interferometer.

3. **The Sample**: Depending on the type of analysis being performed, the beam enters the sample compartment and is transmitted through or reflected off the surface of the sample. This is where the sample's specific frequencies of energy, which are unique to it, are absorbed.

4. **The Detector**: The beam finally reaches the detector, where it is measured. The detectors used were created specifically to measure the interferogram signal.

5. **The Computer**: The measured signal is digitized and sent to the computer, which performs the Fourier transformation. The user is then presented with the final infrared spectrum for interpretation and any further manipulation.

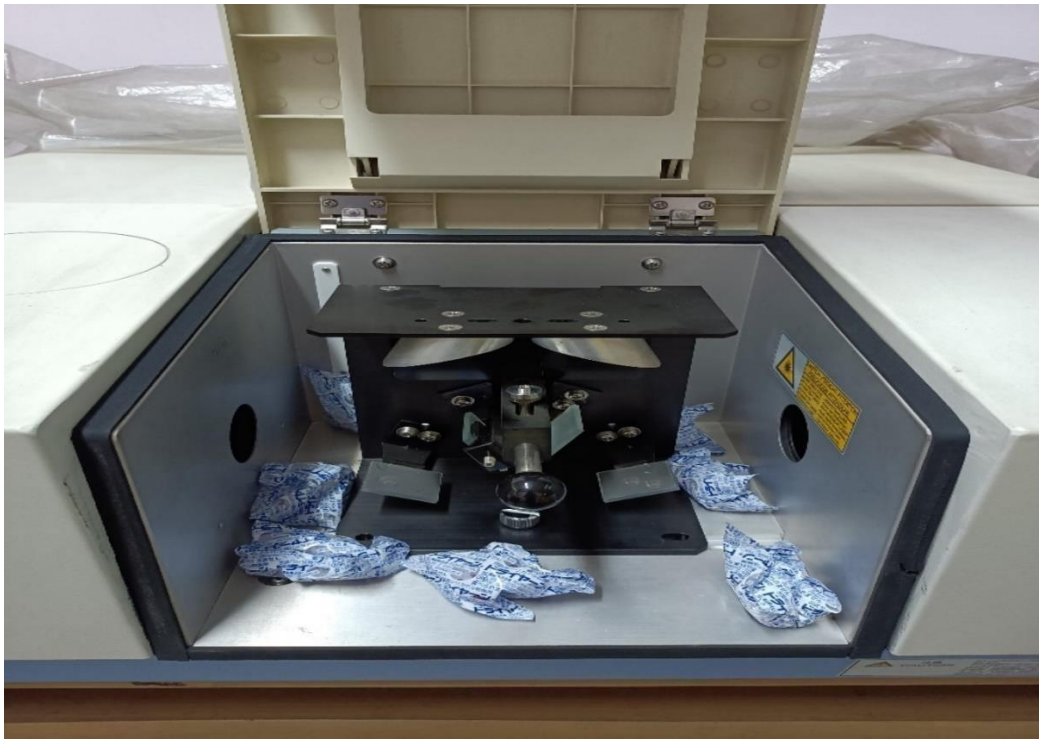


Fig 2.13. Internal components of FTIR instrument.

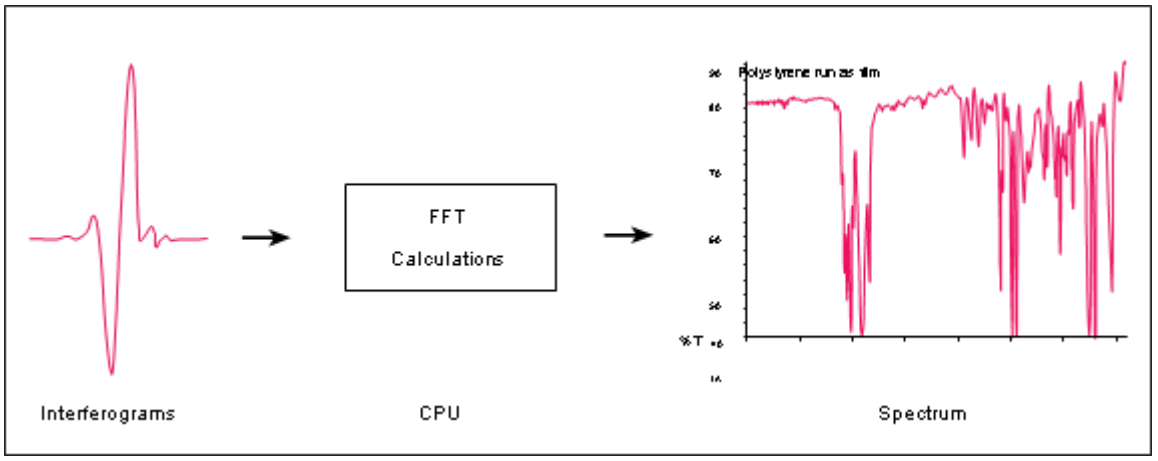


Fig 2.14. Internal Process for the formation of FTIR spectra

Because the absorption intensity must be measured on a relative scale, a background spectrum must also be measured. Normally, this is a measurement without a sample in the beam. This can be compared to the "percent transmittance" measurement taken with the sample in the beam. This method yields a spectrum that is devoid of all instrumental characteristics. As a result, all spectral features present are solely due to the sample. Because the instrument's spectrum is characteristic, a single background measurement can be used for multiple sample measurements.

I-V characterization:

The techniques for the measurement of the electrical behavior of laminated composites are the two- probe method and four probe methods. The two-probe method is based on the definition of resistance when two electrodes are used to measure the electrical resistance. Figure below shows a specimen, on which a pair of contacts (probe 1 and probe 2) with conductive wires is attached. Two probes are used for the electrical current input, as well as for the voltage measure. The resistance of the segment between the voltage contacts can be calculated through Ohm's law:

$$V = I * R$$

where, V and I are the voltage and current from the voltage and current contacts, resp

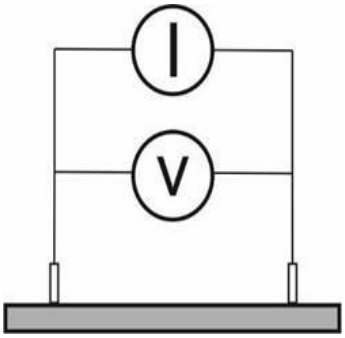
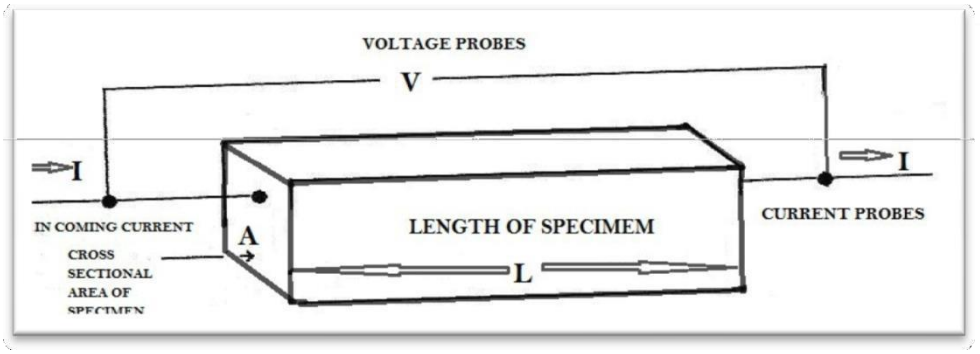


Fig 2.15. Electrical resistivity measurement by two probe method



(a)



(b)

Fig2.16. (a, b) Two probe device used in the project.

● References:

1. Z. Yang, Z. Z. Ye, Z. Xu and B. H. Zhao, "Effect of the Morphology on the Optical Properties of ZnO Nanos tructured," Physica E: Low-Dimensional Systems and Nanostructures, Vol. 42, No. 2, December 2009, pp. 116- 119. doi: 10.1016/j.physe.2009.09.010.
2. Thermo Nicolate, Introduction to Fourier Transform Infrared Spectrometry, © 2001 Thermo Nicolet Corporation.
3. Kortüm, G. Reflectance Spectroscopy: Principles, Methods, Applications; Kortüm, G., Ed.; Springer: Heidelberg/Berlin, Germany, 1969.
4. Frei, R.W.; Frodyma, M.M.; Lieu, V.T. Diffuse reflectance spectroscopy. In Instrumentation for Spectroscopy. Analytical Atomic Absorption and Fluorescence Spectroscopy. Diffuse Reflectance Spectroscopy; Svehla, G., Ed.; Wilson & Wilson's Comprehensive Analytical Chemistry; Elsevier Scientific Publishing Company: Amsterdam, The Netherlands, 1975; Volume 4, Chapter 3, pp. 263–345.
5. Höpe, A. Diffuse Reflectance and Transmittance. In Spectrophotometry: Accurate Measurement of Optical Properties of Materials; Germer, T.A., Zwinkels, J.C., Tsai, B.K., Eds.; Experimental Methods in the Physical Sciences; Academic Press Elsevier Inc.: Amsterdam, The Netherlands, 2014; Volume 46, Chapter 6, pp. 179–219.
6. Lambert, J.H. Lambert's Photometrie. Photometria Sive De Mensura Et Gradibus Luminis, Colorum et Umbrae (1760); Anding, E., Ed.; Ostwald's Klassiker der exakten Wissenschaften; Verlag von Wilhelm Engelmann: Leipzig, Germany, 1892; Volume 31.
7. Bouguer, P. Traité d'optique sur la gradation de la lumiere; I'Abbé de la Caille, M., Ed.; De l'Imprimerie de H.L. Guerin & L.F. Delatour: Paris, France, 1760.
8. Ångström, K. Ueber die Diffusion der strahlenden Wärme von ebenen Flächen. Ann. Phys. 1885, 262, 253–287. [CrossRef]
9. Messerschmitt, J.B. Ueber diffuse Reflexion. Ann. Phys. 1888, 270, 867–896. [CrossRef]
10. Seeliger, H. Zur Photometrie zerstreut reflectirender Substanzen. In Sitzungsberichte der Mathematisch-Physikalischen Classe der k. b. Akademie der Wissenschaften zu München; Franz, G., Ed.; Verlag der K. Akademie: Munich, Germany, 1888; Volume 18, pp. 201–248.
11. Lommel, E. Die Photometrie der diffusen Zurückwerfung. Ann. Phys. 1889, 272, 473–502. [CrossRef]
12. Uljanin, W. Ueber das Lambert'sche Gesetz und die Polarisation der schief emittirten Strahlen. Ann. Phys. 1897, 298, 528–542. [CrossRef]
13. Wright, H. Die diffuse Reflexion des Lichtes an matten Oberflächen. Ann. Phys. 1900, 306, 17–41. [CrossRef]
14. Pokrowski, G.I. Zur Theorie der diffusen Lichtreflexion. Z. Phys. 1924, 30, 66–72. [CrossRef]
15. Schulz, H. Untersuchungen über die Reflexion a teilweise lichtzerstreuenden Flächen. Z. Phys. 1925, 31, 496–506. [CrossRef]
16. Harrison, V.G.W. The light-diffusing properties of magnesium oxide. Proc. Phys. Soc. 1946, 58, 408–419. [CrossRef]
17. Torrent, J.; Barrón, V. Diffuse Reflectance Spectroscopy. In Methods of Soil Analysis Part 5–Mineralogical Methods; Number 5 in the Soil Science Society of America Book

Chapter-3

Different Synthesis Techniques



⁃ Synthesis Techniques:

Carbonaceous materials such as graphite, graphene, graphene oxide (GO) and reduced graphene oxide (rGO) have a huge interest in the new days industry due to their huge range of different applications in different fields of new technology. These materials have a rich synthesis history of 150 years. With time the synthesis procedure indulging these materials upgraded itself with bulk production and less hazards. There are multiple synthesis processes to produce graphene oxide (GO) from graphite and then reducing it into rGO. The past has revealed three main techniques for producing graphene oxides: Staudenmaier's (ST) method, which employs a chlorate oxidant in fuming nitric acid; Hofmann's (HO) version, which uses chlorate in sulfuric acid; and Hummers' (HU) technique which employs a permanganate oxidant. ST method and Hummer's method for synthesis of GO are being discussed in this chapter. The rGO can be produced using this already produced GO by hydrothermal process. Brief description of the hydrothermal process is also included in this chapter.

Numerous methods have been developed to fabricate Si nanostructures as well using top-down or bottom-up approaches, such as vapor-liquid-solid (VLS) growth, reactive ion etching (RIE), electrochemical etching, solution-liquid-solid (SLS) process, chemical vapor deposition (CVD), molecular beam epitaxy (MBE) or metal-assisted chemical etching, all of which aim to control various parameters of the Si structures. In this chapter we have discussed two techniques namely, Chemical Etching and VLS process, in detail.

▪ GO synthesis using Staudenmaier's (ST) method:

Materials: Graphite, Sulphuric acid (H_2SO_4), Nitric acid (HNO_3) and Potassium chlorate ($KClO_3$).

Process:

1. At first sulphuric acid and nitric acid are added to a reaction flask containing a magnetic bit for stirring.
2. Then the solution is cooled at 0^0 C for 10 to 15 minutes.
3. After cooling the solution, graphite is added to the mixture under vigorous stirring so

4. Once the graphite is dispersed into the acid mixture, potassium chlorate is poured into the solution very carefully and slowly at 0^0 C to avoid sudden increase in temperature and production of chlorine dioxide which is very much explosive at high concentration.
5. After the potassium chlorate has completely dissolved, the reaction flask is loosely sealed to enable gas evolution, and the mixture is rapidly agitated for a lengthy amount of time (80 to 100 hours) at room temperature.
6. The mixture is placed into ultra-pure water and then filtered when the reaction is finished.
7. To remove sulfate ions, the GO is then redistributed and repeatedly rinsed with HCl solutions.
8. Finally, the GO is cleaned with ultra-pure water until the filtrate's pH is neutral. Before usage, the slurry GO is then dried for five to seven days at 50^0 C in a vacuum oven.

- ## GO synthesis using Hummers' (HU) method:

Materials: Graphite, concentrated sulphuric acid (H_2SO_4), Sodium Nitrate ($NaNO_3$), Hydrogen peroxide (H_2O_2) and Potassium Permanganate ($KMnO_4$).

Process:

1. To start the reaction, at first graphite is stirred with H_2SO_4 in a reaction flask for a few minutes at 0^0 C so that it can be dispersed into the solution.
2. After that sodium nitrate is added to the mixture in some portions and kept for 1 hour under stirring.
3. Then potassium permanganate is poured slowly into the solution at 35^0 C which eventually raises the temperature to 90^0 C. The temperature is maintained the same for the next 1 hour.
4. Extra water is added to the solution followed by pouring of H_2O_2.
5. Once the solution ends its reaction, it is washed multiple times with warm water.
6. To separate the solid GO, the mixture was then centrifuged multiple times and the solid GO was collected.
7. The solid GO then dried in a vacuum oven for some days before use.

- **Hydrothermal Process:**

The hydrothermal synthesis was defined in the literature as a process in a closed system, in which chemical reactions take place exclusively in a water solvent at increased temperatures, at a pressure that is higher than atmospheric pressure (P > 101,325 Pa). This definition is often modified by scholars, e.g., Byrappa and Yoshimura
[2] proposed a definition of the "hydrothermal reaction" as any heterogeneous chemical reaction in the presence of a solvent (whether aqueous or non-aqueous) above the room temperature and at a pressure greater than 1 ATM in a closed system. For the purposes of this review, we assume that the "hydrothermal synthesis" is a process occurring in an aqueous environment (where $mH_2O > 50\%$), with the pressure equal to or higher than atmospheric pressure. In hydrothermal processes, reaction products are mainly oxides and salts due to the properties of water as a solvent.

Solvothermal synthesis is a method for preparing a variety of materials such as metals, semiconductors, ceramics, and polymers. The process involves the use of a solvent under moderate to high pressure (typically between 1 ATM and 10,000 ATM) and temperature (typically between 100 °C and 1000 °C) that facilitates the interaction of precursors during synthesis. If water is used as the solvent, the method is called 'hydrothermal synthesis'. The synthesis under hydrothermal conditions is usually performed below the supercritical temperature of water (374 °C). The process can be used to prepare structures including various morphologies including thin films, bulk powders, single crystals, and nanocrystals.

In addition, the morphology (sphere (3D), rod (2D), or wire (1D)) of the crystals formed is controlled by manipulating the solvent supersaturation, chemical of interest concentration, and kinetic control. The method can be used to prepare thermodynamically stable and metastable states including novel materials that cannot be easily formed from other synthetic routes .

- **ADVANTAGES OF THE HYDROTHERMAL METHOD**:

i) Possible to precipitate powders directly from solution
ii) Ability to synthesize crystals of substances which are unstable near melting point
iii) Suitable when it is difficult to dissolve precursors at room or lower temperatures

- **DISADVANTAGES OF THE HYDROTHERMAL METHOD:**

i) High cost of equipment e.g., the need of expensive autoclaves.

ii) II. Inability to observe the crystals in the process of their growth

- **REDUCTION OF GO TO rGO:**

The prepared GO can be reduced to remove most of the edge linked functionalization groups to form a pure layer of graphene oxide with less groups (eventually called as reduced graphene oxide) using hydrothermal methods. As hydrothermal or solvothermal techniques possess constant temperature and pressure, thus, effectively the reduction can be done easily in less time. The reduction can include doping as well which is an extra hand of using hydrothermal processes. Different amide groups, sulfur groups etc. can be used as reduction agents. Nitrogen, sulfur, boron etc. can be doped by tuning the components of the reaction.

In this project work, modified Hummer's method is being used for producing good quality of graphene oxide (GO) and rGO is synthesized using a hydrothermal process.

References:

1. Henglein, A. Small-particle research-physicochemical properties of extremely small colloidal metal and semiconductor particles. Chem. Rev. 1989, 89, 1861–1873.
2. Trindade, T.; O'Brien, P.; Pickett, N.L. Nanocrystalline semiconductors: Synthesis, properties, and perspectives. Chem. Mater. 2001, 13, 3843–3858.
3. Kuchibhatla, S.; Karakoti, A.S.; Bera, D.; Seal, S. One dimensional nanostructured materials. Prog. Mater. Sci. 2007, 52, 699–913.
4. Bera, D.; Kuiry, S.C.; Seal, S. Synthesis of nanostructured materials using template-assisted electrodeposition. JOM 2004, 56, 49–53.
5. P. Wick, A. E. Louw-Gaume, M. Kucki, H. F. Krug, K. Kostarelos, B. Fadeel, K. A. Dawson, A. Salvati, E. Vazquez, L. Ballerini, M. Tretiach, E. Flahaut, L. Gauthier, M. Prato and A. Bianco, Classification framework for graphene-based materials, Angew. Chem., Int. Ed., 2014,53(30), 7714–7718.
6. M. I. Katsnelson, Graphene: Carbon in two dimensions, Mater. Today, 2007, 10(1–2), 20–27.
7. S. Alwarappan and A. Kumar, Graphene-based materials: Science and Technology, Chapter 1: Graphene an introduction, Taylor & Francis group, CRC Press, London, New York 2014.
8. K. Deshmukh and G. M. Joshi, Embedded capacitor applications of graphene oxide reinforced poly(3,4-ethyl)-tetramethacrylate(PEDOT-TMA)composites, J.Mater.Sci.:Mater. Electron., 2015, 26, 5896–5909.
9. G. J. Thangamani, K. Deshmukh, K. K. Sadasivuni, K. Chidambaram, M. B. Ahamed, D. Ponnamma, M. A. A. AlMaadeed and S. K. K. Pasha, Recent advances in electrochemical biosensor and gas sensors based on graphene and carbon nanotubes (CNT) – a review, Adv. Mater. Lett., 2017, 8, 196–205.
10. K. K. Sadasivuni, D. Ponnamma, S. Thomas and Y. Grohens, Evolution from graphite to graphene elastomer composites, Prog. Polym. Sci., 2014, 39(4), 749–780.
11. K. Deshmukh, M. B. Ahamed, S. Sankaran, S. K. K. Pasha, K. K. Sadasivuni, D. Ponnamma and M. A. A. AlMaadeed, Studies on the mechanical, morphological and electrical properties of highly dispersible graphene oxide reinforced polypyrrole and polyvinyl alcohol blend composites, Mater. Today: Proc., 2018, 5, 8744–8752.

12. K. Deshmukh, S. Sankaran, M. B. Ahamed, S. K. K. Pasha, K. K. Sadasivuni, D. Ponnamma and M. A. A. AlMaadeed, Studies on the electrical properties of graphene oxide reinforced poly(4-styrene sulfonic acid) and polyvinyl alcohol blend composites, Int. J. Nanosci., 2018, 17, 1760005–1760013.
13. Gao, Wei.Springer, Cham, 2015. 61-95
14. Chan WC, Maxwell DJ, Gao X, Bailey RE, Han M: Luminescent quantum dots for multiplexed biological detection and imaging. Curr Opin Biotechnol 2002, 13(1):40–46.
15. https://www.nanowerk.com/what_are_quantum_dots.php#:~:text=Quantum%20dots%20(QD s)%20are%20man,cells%20and%20fluorescent%20biological%20labels.
16. Xia C., Zhu S., Feng T., Yang M., Yang B. Evolution and synthesis of carbon dots: From carbon dots to carbonized polymer dots. Adv. Sci. 2019;6:1901316. doi: 10.1002/advs.201901316.
17. Namdari P., Negahdari B., Eatemadi A. Synthesis, properties and biomedical applications of carbon-based quantum dots: An updated review. Biomed. Pharmacother. 2017;87:209–222. doi: 10.1016/j.biopha.2016.12.108.
18. Sahu S., Behera B., Maiti T.K., Mohapatra S. Simple one-step synthesis of highly luminescent carbon dots from orange juice: Application as excellent bio-imaging agents. Chem. Commun. 2012;48:8835–8837. doi: 10.1039/c2cc33796g.
19. Atabaev S. Size-tunable carbon nanoparticles with excitation-independent fluorescent properties. Mater. Today Proc. 2017;4:4896–4899. doi: 10.1016/j.matpr.2017.04.092.
20. De B., Karak N. A green and facile approach for the synthesis of water-soluble fluorescent carbon dots from banana juice. RSC Adv. 2013;3:8286–8290. doi: 10.1039/c3ra00088e.
21. Zhou M., Zhou Z., Gong A., Zhang Y., Li Q. Synthesis of highly photoluminescent carbon dots via citric acid and Tris for iron(III) ions sensors and bioimaging. Talanta. 2015;143:107–113.
22. Zhou J., Shan X., Ma J., Gu Y., Qian Z., Chen J., Feng H. Facile synthesis of P-doped carbon quantum dots with highly efficient photoluminescence. RSC Adv. 2014;4:5465–5468. doi: 10.1039/c3ra45294h.
23. Dong Y., Pang H., Yang H.B., Guo C., Shao J., Chi Y., Li C.M., Yu T. Carbon-based dots co-doped with nitrogen and sulfur for high quantum yield and excitation-independent emission. Angew. Chem. Int. Ed. 2013;52:7800–7804. doi: 10.1002/anie.201301114.

Chapter-4

Literature review



WRITING A

THESIS LITERATURE REVIEW

Over the past two decades, research on 2D materials has witnessed a remarkable increase after Geim and Novoselov ground-breaking experiments in 2004 and the discovery of graphene. Since then, based on its exceptional physical characteristics, graphene has become prominent in various research areas of nanoscience and condensed matter physics/chemistry, significantly contributing to a wide range of interdisciplinary fields. Accordingly, the large-scale preparation of graphene-based materials has gained extensive consideration, leading to cutting-edge research and innovative technologies. Concurrently, various enterprises and manufacturers have contributed to the industrialization of graphene. Furthermore, due to its physicochemical characteristics and wide spectrum of applications, interest in graphene has shifted beyond academics to scientific research and industry. However, its susceptible nature to oxidative environments, evidence of certain toxicity, and ideal conductive characteristics, which make it unswitchable, are the primary shortcomings of this wonder material. Thus, the initial enthusiasm created by the "graphene rush" has shifted to exploring more stable and atomically thin materials. Examples of this type of layered materials are boron nitride, recently discovered class of materials (*e.g.*, MXenes) composed of transition metal carbonitrides, nitrides, and carbides,semiconducting transition metal dichalcogenides (TMDCs), and phosphorene. presents some of the principal advancements and recent discoveries in the field of 2D materials. Several pioneering discoveries regarding liquid phase exfoliation are also discussed, including biomedical and sensing applications. The wide range of physical and chemical properties of 2D materials shows significant possibilities for applied research, given that their properties are dependent on their dimensionality. Further, various optoelectronic characteristics can be realized, ranging from the extraordinary semi-metal conductivity of graphene to the semiconducting properties of certain TMDCs. These TMDCs provide a tunable bandgap energy with easy conversion from bulk materials (indirect-form) to single-layered materials (direct-form). These properties result in distinct photoluminescence (PL) characteristics, thus permitting diverse applications, *e.g.*, electroluminescent devices, photodetectors, luminescent probes, and transistors. Furthermore, chemical functionalization can offer desirable optoelectronic properties in the above-mentioned 2D materials. For example, due to their large surface/volume ratio, their demand has increased in the field of sensing and broadened their application area from the quantitative determination of heavy metal ions (*e.g.*, Cd2+, Pb2+, As3+, and Hg2+), gasses (*e.g.*, NH3), and ultrasensitive detection of essential biomolecules (*e.g.*, DNA and proteins) to single molecule detection and beyond. Notably, 2D material-based sensors do not possess intrinsic properties to interact with target molecules selectively. Thus, it is possible to manipulate the interaction between 2D nanosheets and molecules/ions by modifying their inherent properties. Chemical adsorption (*i.e.*, chemisorption) of interacting substances *via* covalent bonds on the basal planes of 2D materials provides significant control of their sensing profile. In contrast,

physical adsorption (*i.e.*, physisorption) of interacting molecules on the basal planes of 2D materials *via* non-covalent interactions is preferred in sensing. These non-covalent interactions offer high recovery rates and are considered promising for real-time monitoring and rapid onsite analysis. Given that physisorption depends on the nature of the molecules and the interacting surface, it has certain limitations. This involves the ineffective and unstable immobilization of molecules, which can potentially cause false positive and negative results. Primarily, a direct electrical response is desirable for practical applications, where the interaction of analytes with 2D materials generates an enticing optical response, for instance, a variation in PL characteristics offers a variety of opportunities. Graphene and its oxide (GO) are known to be effective fluorescence quenchers compared to organic substances. Hence, Förster resonance energy transfer (FRET) sensors have attracted significant attention in recent years, particularly in biomedical applications. Generally, in biomedical applications, FRET can detect *in vitro* and *in vivo* changes and be used to precisely measure nanometer-scale distances. This has resulted in the development of nano-biosensors with exceptional selectivity, increased bio-stability, and improved sensitivity. In this regard, single-layer MoS2 nanosheets with superior fluorescence quenching efficiency are a suitable sensing platform for small molecule determination and DNA detection.The use of 2D materials in FRET sensors is not limited to energy acceptors. Alternatively, suitable functionalization produces photoluminescent flakes, which act as energy donors, and thus quenched by electron-deficient compounds, *e.g.*, for the detection of trinitrophenol, which is an integral component of intense explosives. Recently, 2D materials have been the focus of research for the fabrication of extremely selective and sensitive sensing devices to detect organic vapors, humidity, and hazardous chemicals. These 2D material-based devices are widely used in emission control, environmental monitoring, and diagnosis. In this regard, a broad spectrum of materials has been developed, ranging from carbon materials to metal oxides and various polymers. Certainly, 2D materials should be highlighted owing to their noteworthy features and potential use.These materials include layered metal oxides, black phosphorus, hexagonal boron nitride (h-BN), pnictogens, TMDCs, and MXenes. Because of their high adsorption capacity and broad surface area, these materials exhibit improved performances for gas sensing. Two configurations of the above-mentioned 2D materials have been utilized in gas sensors, *i.e.*, field-effect transistors (FETs) and chemiresistors. Because of their ease of attachment, point-of-care sensing, and the ability to construct compact wearable electronic devices, 2D materials have become superior technology for assessing human physiological signals.

Saliva detection. Besides being one of the most prevalent chemical samples, saliva, together with sweat and tears, contains a broad range of biomarkers that are the same as that in the blood.

Furthermore, the high volume of saliva fluid and big mouth cavity are both favorable for sample collection and sensor localization. However, although there have been some studies on saliva sensors to detect glucose and lactate, the application of 2D materials in saliva inspection remains rare Using a live saliva sample, Mannoor *et al.* introduced a wireless sensor composed of elastic graphene and silk, which was sufficiently flexible to be worn on the finger and employed to detect bacteria in dental enamel. Antimicrobial peptides were added to the surface of graphene to enable the detection of harmful bacteria over a vast range and time on the material surface. The signals generated by the bacterium concentration could be sent to an external device without requiring an external power source by combining a sensing area of graphene using an inductive coil antenna Also, it was possible to connect it to tissues or tooth enamel because of the water-soluble and biocompatible silk substrate. The results indicate that monitoring bacteria in the mouth is effective because there is a linear correlation between the logarithm of bacteria content and the variation in resistance. Recently, Liao *et al.* developed flexible organic electrochemical transistors for the determination of glucose and uric acid in saliva, which was capable of withstanding considerable deformation Immobilization of the enzyme uricase (UO*x*) on the surface of graphene was performed for the selective detection of uric acid. The positively and negatively charged double layer of Pt-gate/Nafion-graphene/PANI/UO*x*-GO could prevent the interaction between uric acid and glucose. According to the results, the proposed device exhibited a detection limit of $\sim 1 \times 10{-}8$ M, which is nearly three times the magnitude and superior to the detection limit of traditional electrochemical techniques.

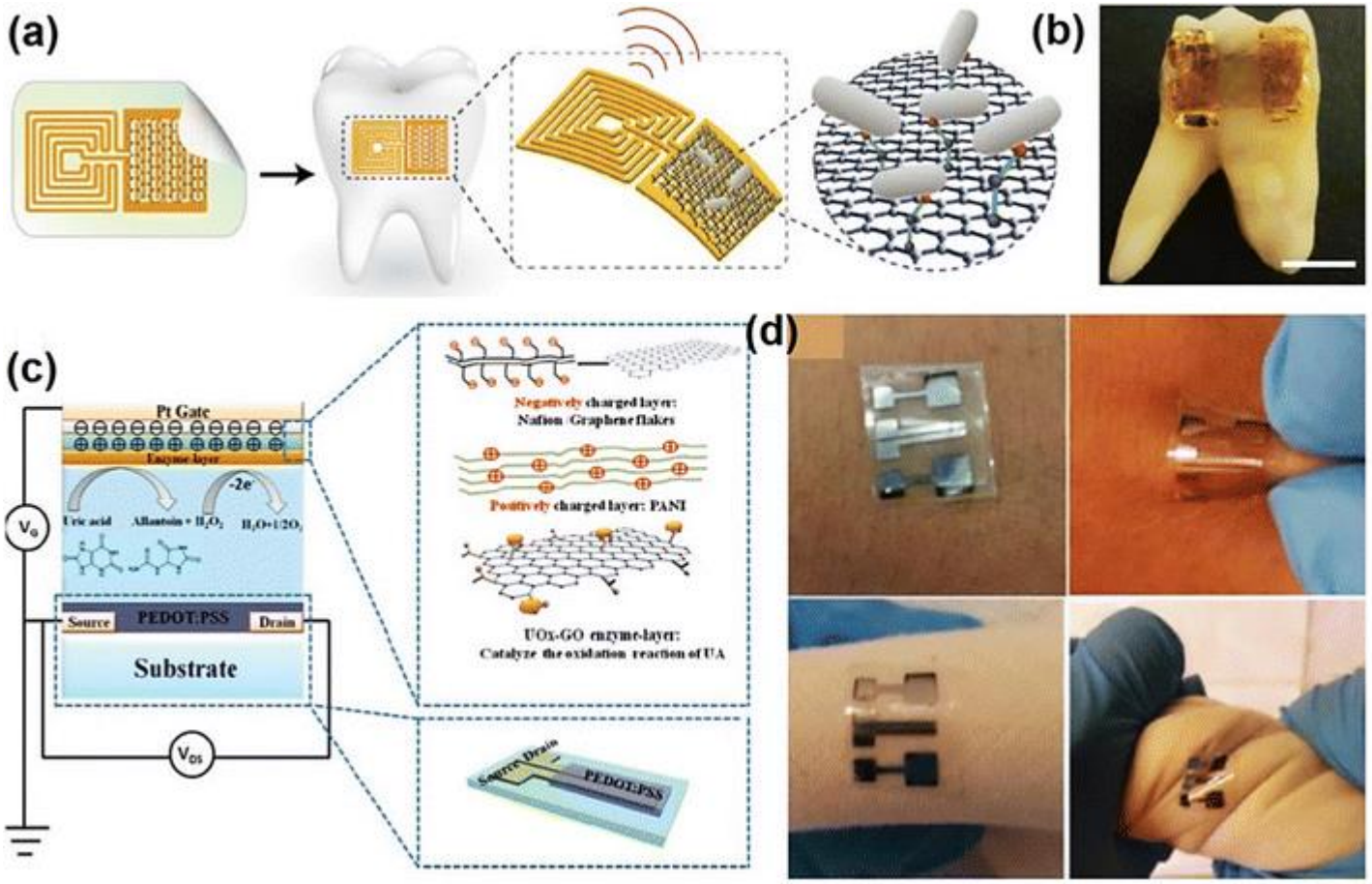


Fig 4.1

Fig. 16 (a) Graphical representation of graphene/silk-based wireless biosensor (mounted on a tooth) for sensing bacteria. (b) Digital photograph of the developed sensor (over tooth surface). Adapted with permission from ref. Copyright 2012, Nature Publishing Group. (c) Schematic of the working mechanism and organic electrochemical transistor with Pt-gate/Nafion-graphene/PANI/UO*x*-GO employed for saliva analysis. (d) Application of proposed sensors on various surfaces. Adapted with permission from ref. Copyright 2015, John Wiley & Sons.

3.6 Biomedical and health care sensors

3.6.1 Single-cell detection. Single sickle cell detection, which distinguishes unhealthy from healthy cells, provides details about the ailment and plays a significant part in diagnosis. Consequently, the reliable identification of single cells is needed amongst healthy cells. Currently, optofluidic

technologies and flow cytometry are the most widely used approaches for on-site single-cell detection. However, these systems have difficulty detecting single cells and require a laser source (high-energy source), which can destroy the cells. Xing *et al.* created a graphene-coupled surface plasmon resonance (SPR) sensor that offers an elevated resolution (1.7 × 10−8) and high sensitivity (4.3 × 107 mV per RIU), and further used for single cell identification of cancer cells in a group of healthy cells.As the input source, a helium-neon (He–Ne) laser (λ = 632.8 nm, P = 80 mW) was utilized, which was then converted into circularly polarized light by a polarizer and quarter-wave plate. A schematic illustration of the graphene-based optical prism sensor (GOPS) is displayed in (inset), possessing a sandwiched structure of quartz over prism, thick h-rGO (8.1 nm), microfluidic chip of polydimethylsiloxane, and cell flow. The optical microfluidic channel possessed a width of ∼20 μm and height of ∼12.5 μm. An improvement in the detection range was achieved *via* a diaphragm using a polarized light (reflected) beam spotted over 1 μm. Subsequently, the obtained beam was allowed to pass *via* a polarization beam splitter (PBS) to isolate the transverse magnetic and electric modes, which were identified through a stable photo-detector.In single-cell detection *via* this experiment, the normal lymphocytes and Jurkat cancer cells (JCCs) (1%) present in the blood could be perceived through the modification of the voltage through a microfluidic device called GOPS.

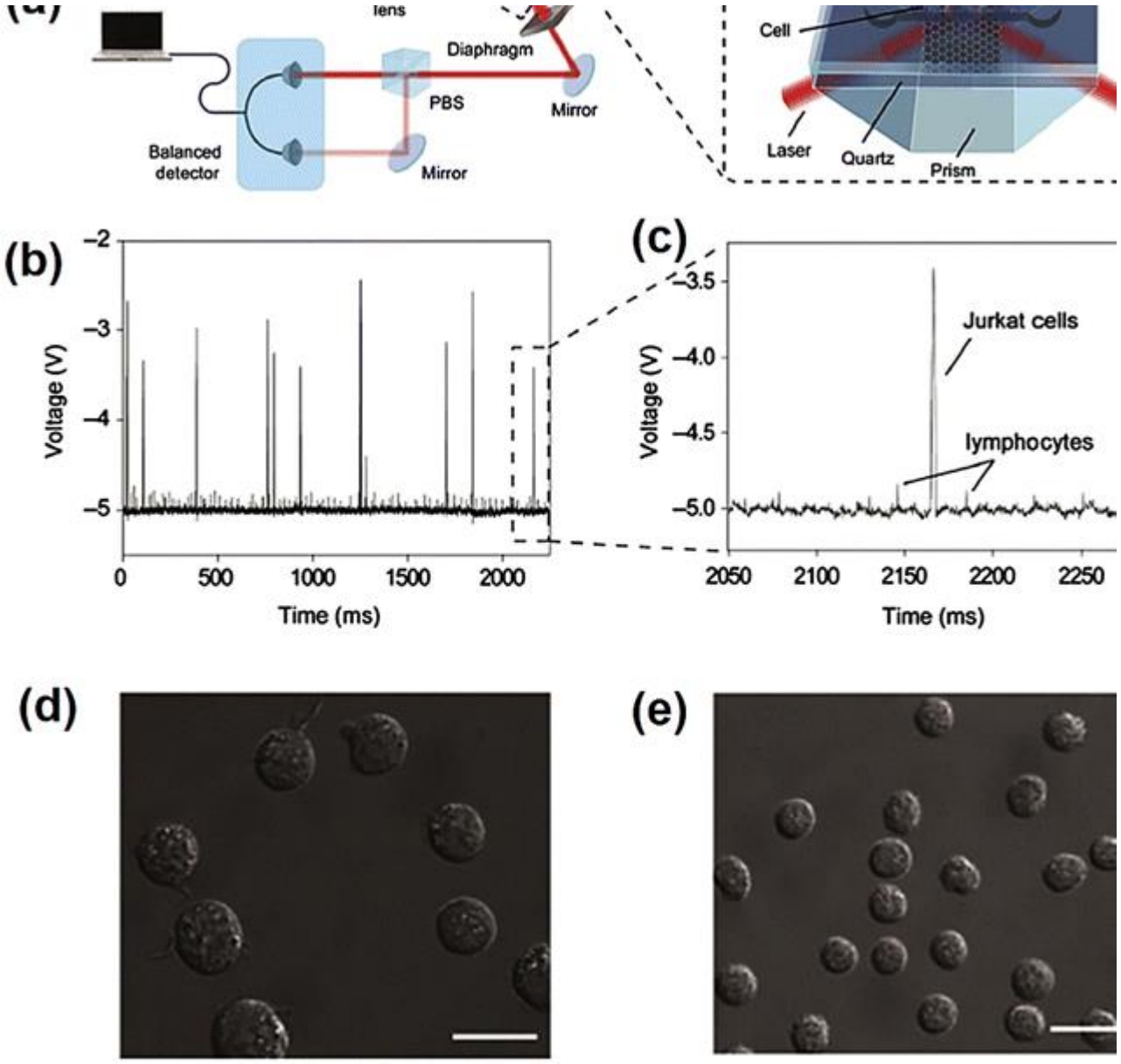


Fig 4.2

Fig. 17 Schematic of optical prism coated with graphene for the ultra-sensitive low detection of distinct cells (a typical SPR system): (a) flow-detecting structure for a single-cell setup, and the inset corresponds to optical sensor platform with graphene-coated for single cell detection, (b) distinct voltage change (time-dependent) agreeing with mixed Jurkat cells and lymphocytes due to their rolling through h-rGO sensing frame and (c) enlarged image of certain positions of the panel (voltage signals are clearly described). Microscopic image (15 μm scale bar) of (d) Jurkat cells and (e) lymphocytes. Adapted with permission from ref.

References

1. K. S. Novoselov, A. K. Geim, S. V. Morozov, D. Jiang, M. I. Katsnelson, I. V. Grigorieva, S. V. Dubonos and A. A. Firsov, *Nature*, 2005, **438**, 197–200 CrossRef CAS PubMed.
2. A. C. Ferrari, F. Bonaccorso, V. Fal'ko, K. S. Novoselov, S. Roche, P. Bøggild, S. Borini, F. H. L. Koppens, V. Palermo, N. Pugno, J. A. Garrido, R. Sordan, A. Bianco, L. Ballerini, M. Prato, E. Lidorikis, J. Kivioja, C. Marinelli, T. Ryhänen, A. Morpurgo, J. N. Coleman, V. Nicolosi, L. Colombo, A. Fert, M. Garcia-Hernandez, A. Bachtold, G. F. Schneider, F. Guinea, C. Dekker, M. Barbone, Z. Sun, C. Galiotis, A. N. Grigorenko, G. Konstantatos, A. Kis, M. Katsnelson, L. Vandersypen, A. Loiseau, V. Morandi, D. Neumaier, E. Treossi, V. Pellegrini, M. Polini, A. Tredicucci, G. M. Williams, B. Hee Hong, J.-H. Ahn, J. Min Kim, H. Zirath, B. J. van Wees, H. van der Zant, L. Occhipinti, A. Di Matteo, I. A. Kinloch, T. Seyller, E. Quesnel, X. Feng, K. Teo, N. Rupesinghe, P. Hakonen, S. R. T. Neil, Q. Tannock, T. Löfwander and J. Kinaret, *Nanoscale*, 2015, **7**, 4598–4810 RSC.
3. M. Chakraborty and M. S. J. Hashmi, *Adv. Mater. Process. Technol.*, 2018, **4**, 573–602 Search PubMed.
4. M. J. Molaei, M. Younas and M. Rezakazemi, *ACS Appl. Electron. Mater.*, 2021, **3**, 5165–5187 CrossRef CAS.
5. M. W. Barsoum, *Prog. Solid State Chem.*, 2000, **28**, 201–281 CrossRef CAS.
6. Q. H. Wang, K. Kalantar-Zadeh, A. Kis, J. N. Coleman and M. S. Strano, *Nat. Nanotechnol.*, 2012, **7**, 699–712 CrossRef CAS PubMed.
7. L. Li, Y. Yu, G. J. Ye, Q. Ge, X. Ou, H. Wu, D. Feng, X. H. Chen and Y. Zhang, *Nat. Nanotechnol.*, 2014, **9**, 372–377 CrossRef CAS PubMed.
8. H. Liu, A. T. Neal, Z. Zhu, Z. Luo, X. Xu, D. Tománek and P. D. Ye, *ACS Nano*, 2014, **8**, 4033–4041 CrossRef CAS PubMed.
9. A. Raza, U. Qumar, A. A. Rafi and M. Ikram, *Sustainable Mater. Technol.*, 2022, **33**, e00462 CrossRef CAS.
10. A. Gupta, T. Sakthivel and S. Seal, *Prog. Mater. Sci.*, 2015, **73**, 44–126 CrossRef CAS.
11. A. S. Mayorov, R. V. Gorbachev, S. V. Morozov, L. Britnell, R. Jalil, L. A. Ponomarenko, P. Blake, K. S. Novoselov, K. Watanabe, T. Taniguchi and A. K. Geim, *Nano Lett.*, 2011, **11**, 2396–2399 CrossRef CAS PubMed.
12. C. Schneider, M. M. Glazov, T. Korn, S. Höfling and B. Urbaszek, *Nat. Commun.*, 2018, **9**, 2695 CrossRef PubMed.
13. N. Zibouche, P. Philipsen, A. Kuc and T. Heine, *Phys. Rev. B: Condens. Matter Mater. Phys.*, 2014, **90**, 125440 CrossRef.

14. J. Wang, I. Verzhbitskiy and G. Eda, *Adv. Mater.*, 2018, **30**, 1802687 CrossRef PubMed.
15. M. Long, P. Wang, H. Fang and W. Hu, *Adv. Funct. Mater.*, 2019, **29**, 1803807 CrossRef.
16. X. Cao, C. Ding, C. Zhang, W. Gu, Y. Yan, X. Shi and Y. Xian, *J. Mater. Chem. B*, 2018, **6**, 8011–8036 RSC.
17. A. Daus, S. Vaziri, V. Chen, Ç. Köroğlu, R. W. Grady, C. S. Bailey, H. R. Lee, K. Schauble, K. Brenner and E. Pop, *Nat. Electron.*, 2021, **4**, 495–501 CrossRef CAS.
18. A. Shahin, K. Ibrahim, F. Ye, R. Karimi, J. Sanderson and K. P. Musselman, *Sens. Actuators, B*, 2022, **359**, 131576 CrossRef CAS.
19. R. Kumar, N. Goel, M. Hojamberdiev and M. Kumar, *Sens. Actuators, A*, 2020, **303**, 111875 CrossRef CAS.
20. Y. Hu, Y. Huang, C. Tan, X. Zhang, Q. Lu, M. Sindoro, X. Huang, W. Huang, L. Wang and H. Zhang, *Mater. Chem. Front.*, 2017, **1**, 24–36 RSC.
21. L.-x. Yu and R.-t. Lv, *New Carbon Mater.*, 2021, **36**, 995–1012 CrossRef CAS.
22. M. Pumera and A. H. Loo, *TrAC, Trends Anal. Chem.*, 2014, **61**, 49–53 CrossRef CAS.
23. U. Qumar, J. Z. Hassan, R. A. Bhatti, A. Raza, G. Nazir, W. Nabgan and M. Ikram, *J. Mater. Sci. Technol.*, 2022, **131**, 122–166 CrossRef.
24. C. Anichini, W. Czepa, D. Pakulski, A. Aliprandi, A. Ciesielski and P. Samorì, *Chem. Soc. Rev.*, 2018, **47**, 4860–4908 RSC.
25. C. Zhu, Z. Zeng, H. Li, F. Li, C. Fan and H. Zhang, *J. Am. Chem. Soc.*, 2013, **135**, 5998–6001 CrossRef CAS PubMed.
26. D. Dinda, A. Gupta, B. K. Shaw, S. Sadhu and S. K. Saha, *ACS Appl. Mater. Interfaces*, 2014, **6**, 10722–10728 CrossRef CAS PubMed.
27. A. Raza, Y. Zhang, A. Cassinese and G. Li, *Catalysts*, 2022, **12**, 1613 CrossRef CAS.
28. J. Z. Hassan, A. Raza, U. Qumar and G. Li, *Sustainable Mater. Technol.*, 2022, **33**, e00478 CrossRef CAS.
29. F. K. Perkins, A. L. Friedman, E. Cobas, P. M. Campbell, G. G. Jernigan and B. T. Jonker, *Nano Lett.*, 2013, **13**, 668–673 CrossRef CAS PubMed.
30. C. Yim, K. Lee, N. McEvoy, M. O'Brien, S. Riazimehr, N. C. Berner, C. P. Cullen, J. Kotakoski, J. C. Meyer, M. C. Lemme and G. S. Duesberg, *ACS Nano*, 2016, **10**, 9550–9558 CrossRef CAS PubMed.
31. Y. Liu, M. Pharr and G. A. Salvatore, *ACS Nano*, 2017, **11**, 9614–9635 CrossRef CAS PubMed.
32. Y. Zang, F. Zhang, C.-a. Di and D. Zhu, *Mater. Horiz.*, 2015, **2**, 140–156 RSC.
33. S. Xu, Y. Zhang, L. Jia, E. Mathewson Kyle, K.-I. Jang, J. Kim, H. Fu, X. Huang, P. Chava, R. Wang, S. Bhole, L. Wang, J. Na Yoon, Y. Guan, M. Flavin, Z. Han, Y. Huang and A. Rogers John, *Science*, 2014, **344**, 70–74 CrossRef CAS PubMed.
34. T. Yamada, Y. Hayamizu, Y. Yamamoto, Y. Yomogida, A. Izadi-Najafabadi, D. N. Futaba and K. Hata, *Nat. Nanotechnol.*, 2011, **6**, 296–301 CrossRef CAS PubMed.
35. S. Chen, Y. Song, D. Ding, Z. Ling and F. Xu, *Adv. Funct. Mater.*, 2018, **28**, 1802547 CrossRef.
36. W. Gao, S. Emaminejad, H. Y. Y. Nyein, S. Challa, K. Chen, A. Peck, H. M. Fahad, H. Ota, H. Shiraki, D.

Chapter-5

Experiments:

Synthesis of Samples



Synthesis of Graphene Oxide (GO) using modified Hummer's method:

- **Materials:**

Graphite flakes (7–10 μm grain size, 99% purity) from Alfa Aesar; sodium nitrate ($NaNO_3$), 99% purity), sulfuric acid (H_2SO_4, 98% by weight, G.R.), potassium permanganate ($KMnO_4$, 99% purity), hydrochloric acid (HCL), hydrogen peroxide (H_2O_2, 30% by weight, A.R.) from Merck were used for synthesis. Deionized (DI) water was taken from a Direct-Q Millipore deionized (18 Ω at 25°C) [

- **Sample Preparation:**

1. Graphene Oxide (GO) was produced through oxidation and exfoliation of graphite flakes using modified Hummer's method. To start the process, at first 3 gm. of graphite powder and 3 gm. of sodium nitrate were mixed well and taken in a 500 ml beaker containing 180 ml concentrated sulphuric acid. This solution underwent vigorous stirring for 2 hours [3].
2. Then, 10 gm. of potassium permanganate were included into the black solution very slowly for 30 minutes keeping the temperature under 15^o C. Again, the solution was kept under vigorous stirring for next 24 hours.
3. Then, to achieve a colour change from black to golden yellow, 200 mL DI and 10 mL 30% H2O2 were gradually added to the solution while maintaining a temperature of roughly 40°C. After that, the mixture was allowed to settle and cool to room temperature [4].
4. The bottom portion of the clear supernatant was decanted, centrifuged twice at 12000 rpm for 15 minutes, washed with 5% hydrochloric acid once, and the resultant supernatant was removed.
5. Following a DI wash, the bottom portion (brown in colour) was centrifuged for 10 minutes at 12000 rpm to create three layers in the centrifuged tube. The middle light brown colour solution was extracted after the upper colourless portion was first removed.
6. The bottom part of the solution having GO and excess graphite, was centrifuged subsequently 5 times and each time the middle portion containing GO was extracted and the lower part was removed .

7. To obtain newly prepared GO, the light brown suspension was dried in a vacuum oven for 24 hours at 48°C.

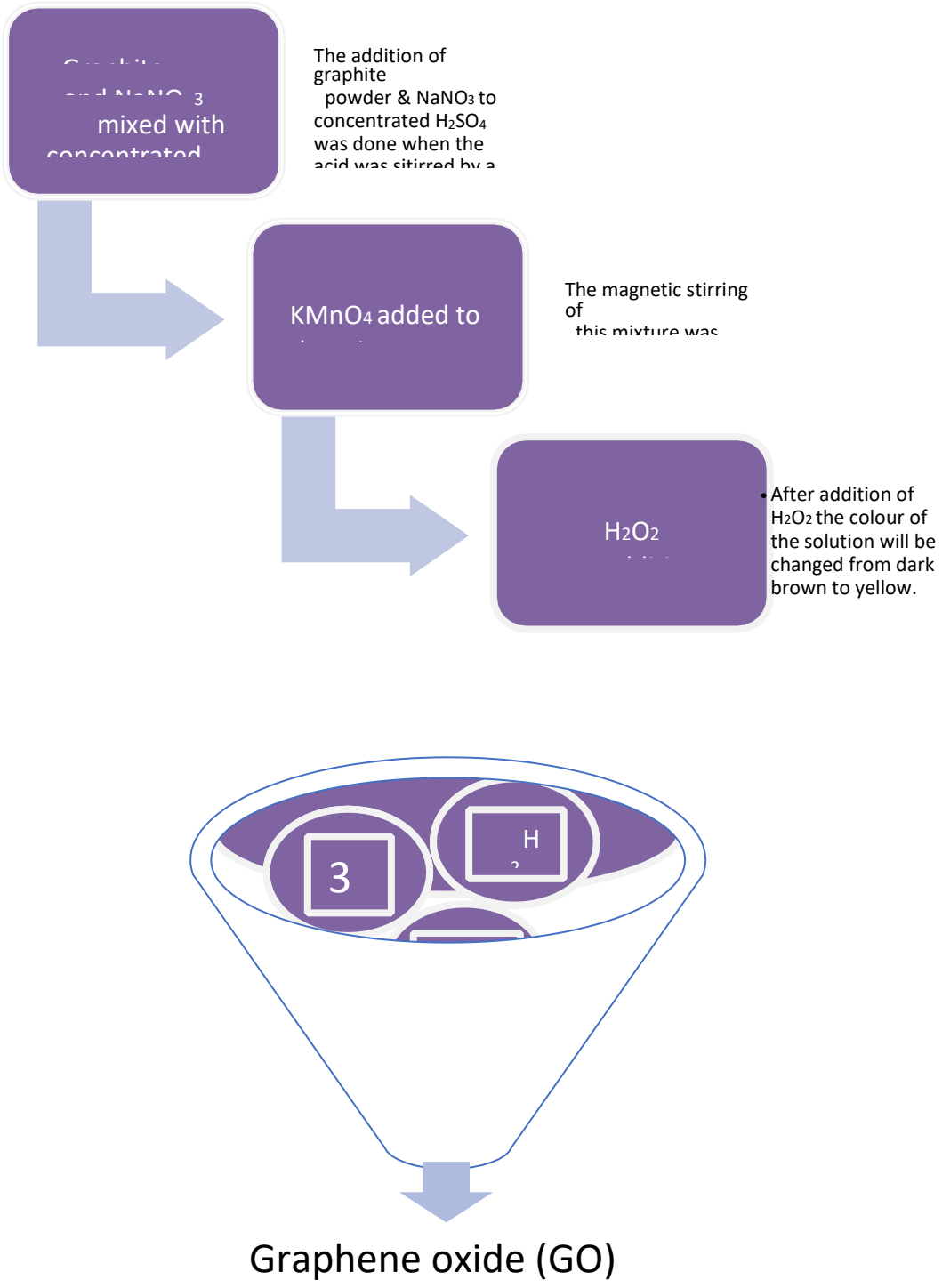


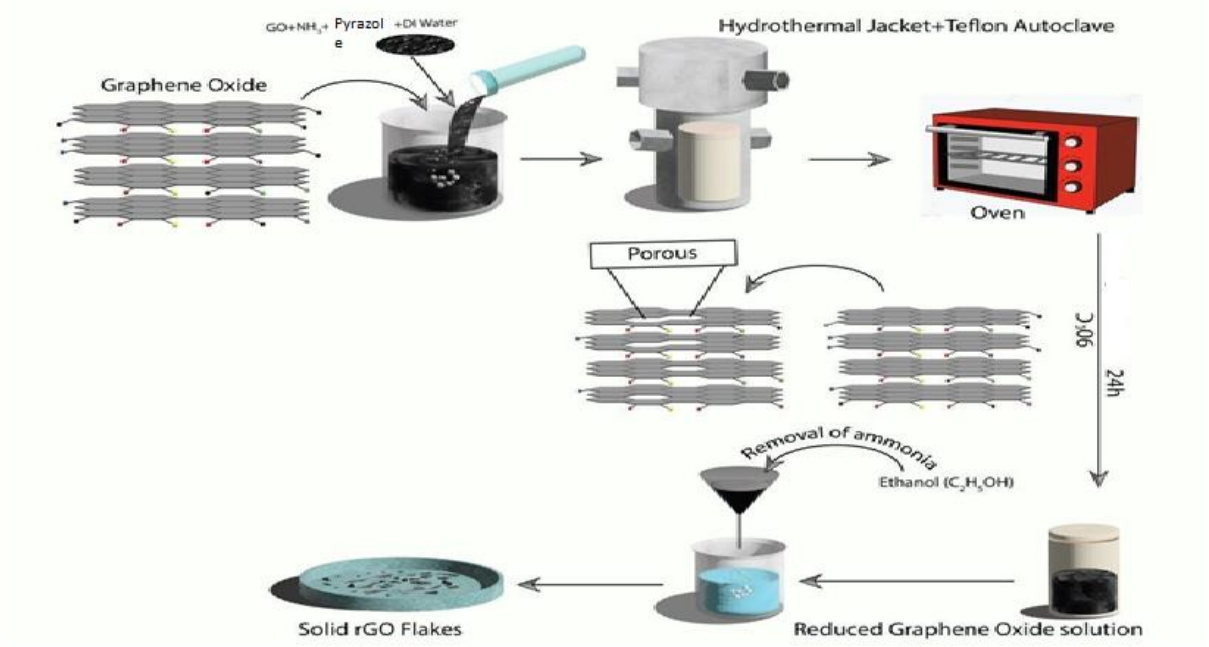
Fig 5.1. Schematic diagram of modified Hummer's method.

Synthesis of N-doped reduced Graphene Oxide (rGO) using hydrothermal method:

- **Materials:** Graphene Oxide (GO) prepared using modified Hummer's method, Imidazole, ethanol (C_2H_5OH, 99% pure), ammonia solution (NH_4OH, 25% by weight), Teflon.

- **Sample preparation:**

1. The already prepared GO from Hummer's method is being reduced to nitrogen doped rGO using in-situ hydrothermal process. At first, 40 mg of fresh prepared GO had been added into 80 ml DI water in a 250 ml beaker and sonicated for 20 minutes so that the solid GO flakes can be dispersed well into DI.
2. After completion of sonication, the mixture was settled down for some time. In the meantime, 20 mg of Pyrazole was weighed and mixed with 10 ml of DI and 10 ml of ammonia solution. This pyrazole-ammonia-DI solution was then mixed with the dispersed GO solution and again sonicated for 10 minutes.
3. A prepared solution was then kept in a Teflon auto-clave and packed tightly into a hydrothermal metal jacket. Finally, the solution was kept in the oven at 90^0 C for 24h comparative study of reduced graphene oxide and the role of nitrogen as a dopant.
4. After completion of the reactions, the solution was kept for getting settled and cooled down to room temperature. Then, the solution was kept into a beaker and also kept into four centrifuge tube to remove excess and unreacted ammonia and then 4 to 5 times centrifugation rpm of 10000 the PH level was came in the neutral then we kept rGO solution into a petri dish and dried at 50 degree C for 24 hours.To obtain fresh solid N-doped rGO flakes.



x

Fig 5.2. Schematic diagram of N-rGO synthesis from GO using hydrothermal process.

References:

[1] A. K. Geim, K. S. Novoselov, *Nat. Mater.* 2007, *6*, 183 –191.

[2] a) C. K. Chua, M. Pumera, *Chem. Soc. Rev.* 2013, *42*, 3222– 3233; b) M. Pumera, *Electrochem. Commun.* 2013, *36*, 14 –18.

L. Staudenmaier, *Ber. Dtsch. Chem. Ges.* 1898, *31*, 1481 –1487.

[3] U. Hofmann, E. König, *Z. Anorg. Allg. Chem.* 1937, *234*, 311 –336.

[4] W. S. Hummers, R. E. Offeman, *J. Am. Chem. Soc.* 1958, *80*, 1339 –1339.[8] C. K. Chua, Z. Sofer, M. Pumera, *Chem. Eur. J.* 2012, *18*, 13453 – 13459.

[9] a) A. Y. S. Eng, A. Ambrosi, C. K. Chua, F. Sˇaneˇk, Z. Sofer, M. Pumera, *Chem. Eur. J.* 2013, *19*, 12673 –12683 ; b) D. C. Marcano, D. V. Kosynkin, J. M. Berlin, A. Sinitskii, Z. Sun, A. Slesarev, L. B. Alemany, W. Lu, J. M.Tour, *ACS Nano* 2010, *4*, 4806 – 4814.

[10]C. K. Chua, M. Pumera, *Chem. Asian J.* 2012, *7*, 1009 –1012.[11] Y. Si, E. T. Samulski, *Chem. Mater.* 2008, *20*, 6792 –6797.

[12] E. Morales-Narváez, A. Merkoçi, *Adv. Mater.* 2012, *24*, 3298 – 3308.

[13] C. Su, M. Acik, K. Takai, J. Lu, S. J. Hao, Y. Zheng, P. Wu, Q. Bao, T. Enoki, Y. J. Chabal, K. Ping Loh, *Nat. Commun.* 2012, *3*, 1298.

[14] a) R. Sitko, E. Turek, B. Zawisza, E. Malicka, E. Talik, J. Heimann, A. Gagor, B. Feist, R. Wrzalik, *Dalton Trans.* 2013, *42*, 5682 –5689 ; b) G. Zhao, X. Ren, X. Gao, X. Tan, J. Li, C. Chen, Y. Huang, X. Wang, *Dalton Trans.* 2011, *40*, 10945 –10952; c) G. Zhao, J. Li, X. Ren, C. Chen, X. Wang, *Envi-ron. Sci. Technol.* 2011, *45*, 10454 –10462; d) C. J. Madadrang, H. Y. Kim, G. Gao, N. Wang, J. Zhu, H. Feng, M. Gorring, M. L. Kasner, S. Hou, *ACS Appl. Mater. Interfaces* 2012, *4*, 1186 – 1193; e) Y. C. Lee, J. W. Yang, *J. Ind. Eng. Chem.* 2012, *18*, 1178 –1185.

[15] F. Han, A. Banin, Y. Su, D. Monts, J. Plodinec, W. Kingery, G. Triplett, *Naturwissenschaften* 2002, *89*, 497 – 504.

[16] L. Järup, *Brit. Med. Bull.* 2003, *68*, 167 – 182.

[17] a) S. Wang, H. Sun, H. M. Ang, M. O. Tadé, *Chem. Eng. J.* 2013, *226*, 336 –347; b) R. Sitko, B. Zawisza, E. Malicka, *TrAC Trends Anal. Chem.* 2013, *51*, 33 –43; c) B. Zawisza, R. Sitko, E. Malicka, E. Talik, *Anal. Methods* 2013, *5*, 6425 –6430.

[18] M. S. Mauter, M. Elimelech, *Environ. Sci. Technol.* 2008, *42*, 5843 –5859.

[19] Y. Wang, S. Gao, X. Zang, J. Li, J. Ma, *Anal. Chim. Acta* 2012, *716*, 112 –118.

[20] Y. Gao, Y. Li, L. Zhang, H. Huang, J. Hu, S. M. Shah, X. Su, *J. Colloid Inter-face Sci.* 2012, *368*, 540 –546.

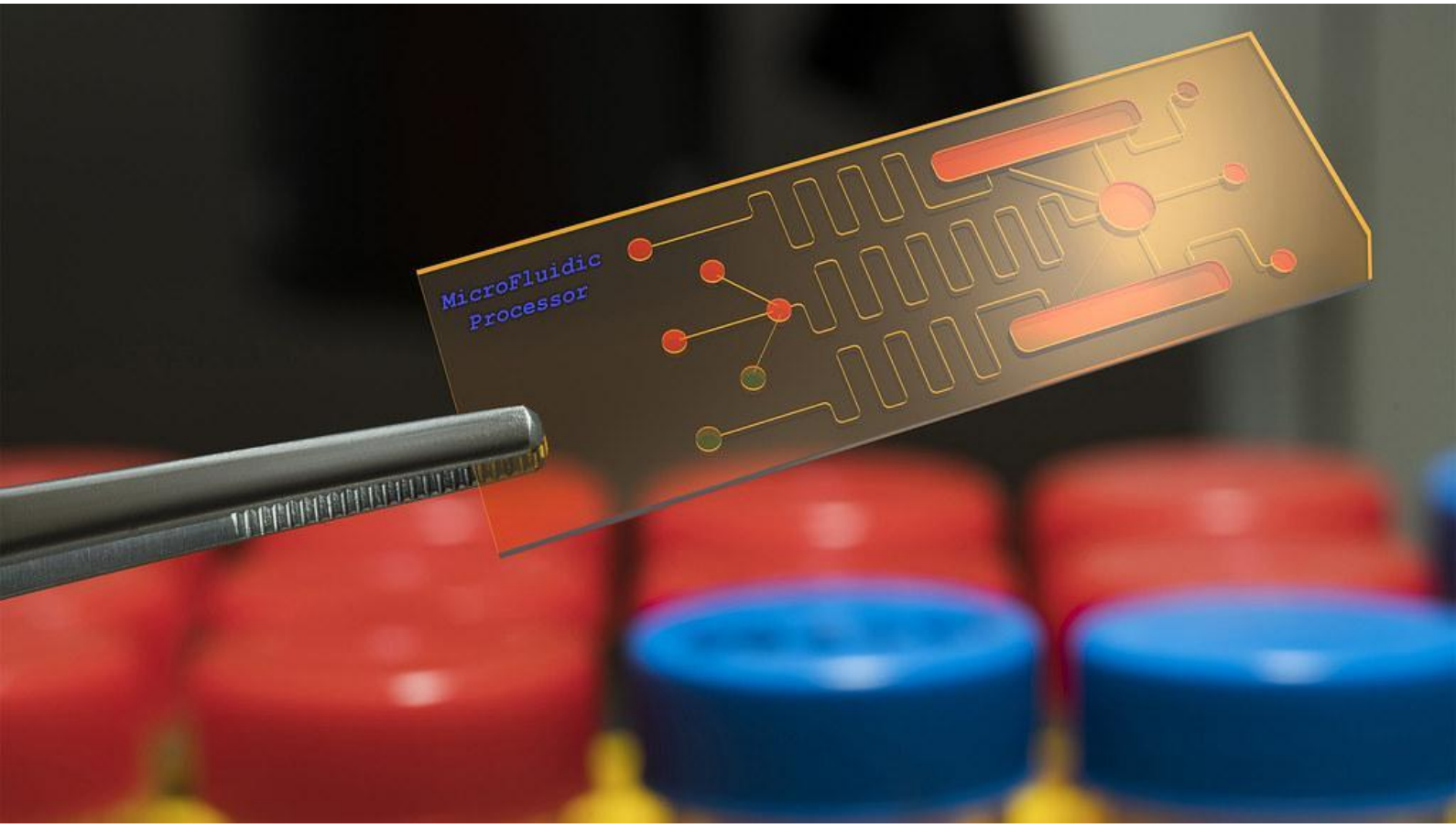
[21] S. T. Yang, S. Chen, Y. Chang, A. Cao, Y. Liu, H. Wang, *J. Colloid Interface Sci.* 2011, *359*, 24 –29.

[22] a) M. Acik, G. Lee, C. Mattevi, A. Pirkle, R. M. Wallace, M. Chhowalla, K. Cho, Y. Chabal, *J. Phys. Chem. C* 2011, *115*, 19761 –19781; b) S. Park, K. S. Lee,leksic´A. .

Chapter-6

Device Fabrication:

Part-I (Biosensor)



Preparation of Ito based Biosensor

A biosensor is an investigative instrument which combines any system with the real sensors to develop a quantitative signal comparable to the analyte's content. In recent decades, a huge quantity of biosensors have been produced for different applications like food, biomedical, and environmental. By considering the different types of sensing methods generally applied in the biosensing process, this chapter focuses on the outline of the present developments in the manufacturing of biosensors depending on electrochemical, medical, optical, and electronics. FTO based biosensor has achieved high scalability, sensitivity and low power consumption with ease of fabrication process. When FTO is used as a Biosensor technology then it increases the detection capability with enhanced specificity and less amount of analyte required.

1. At first the dimension of 1*1(length by width) cm of FTO substrate was made from the large FTO substrate.
2. Then both sides of the substrate were coated by Kapton tape and the length of 0.25 cm and not coating in the middle of the substrate for .5 cm.
3. In the meantime, the FTO substrate was washed by Ethanol ,Acetone and DI water for 15 minutes consecutively . Then the middle part of the substrate was etched by HCL and Zinc by gently rubbing by the tip of the spatula. Using the same technique, 3 pet substrate were being prepared with 3 different types of pet substrate with 1 layer ,2 layer, 3 layer by the same sample and also prepared another set of 3 different type of 1,2,3 layered of pet substrate with the 1 layer coating of GOX enzyme for comparative study.

⁃ Preparation of Multiple layer of Rgo based Biosensor:

1st set of 3 different type pet substrate were being prepared then 1mg of rGO sample was kept into DMF solution and then sonicated into a sonication machine for 15 to 20 minutes.

After the this rGO solution kept into a T20 micro pipet by using the pipet the one droplet of rGO DMF solution was put on pet substrate then the substrate was kept into Spin Coating machine at the Rpm of 3000 and spinning time was 30 sec then completing the spinning the substrate was kept on Hot Plate machine and doing this process the 1 layer of rGO pet substrate was prepared after doing the same Process we have done 2 and 3 layer rGO pet substrates.

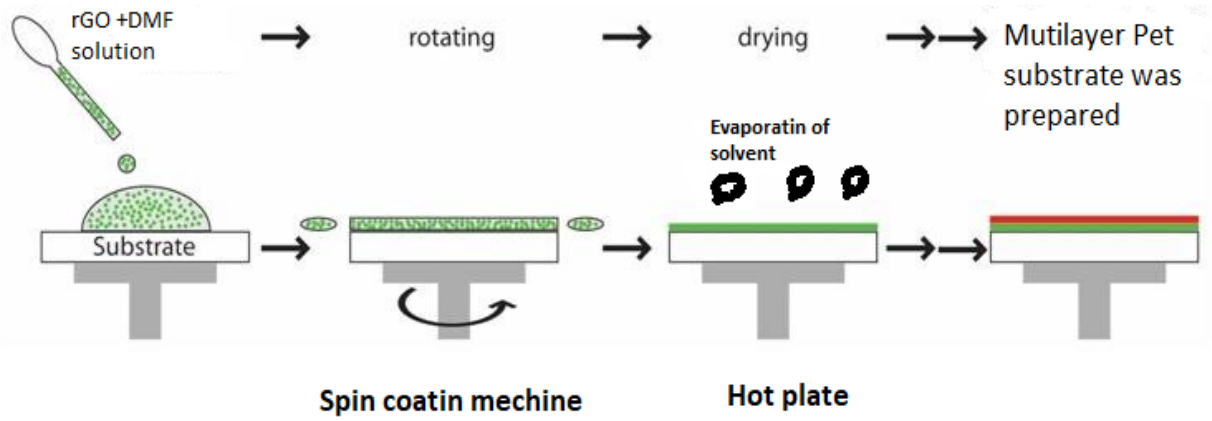


Fig 6.1: **diagram of of rGO coated in PET substrate Fabrication process**

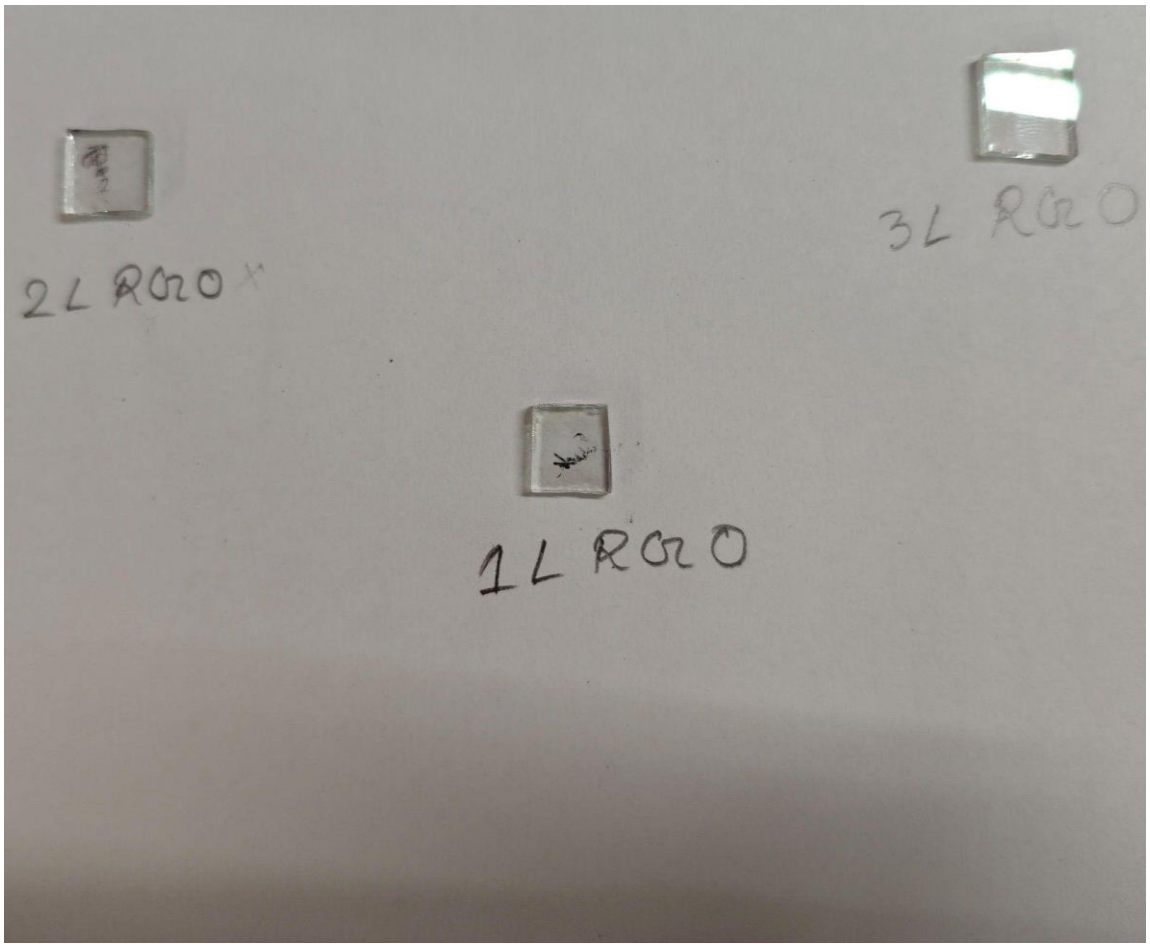


FIG 6.2: Digital photograph of Multiple layer rGO based PET substrate

Preparation of Multiple layer of rGO_Gox based Biosensor

Step-1 Undergoing the same process of making 1,2,3 layer of pet substrate now 0.1 mg GOX enzyme was kept into 10 ml deionized water and then the solution was kept into sonication machine for 15 minutes .Then the solution was kept into the micropipette of T20 then one droplet of gox solution was put on rGO coated pet

substrate then getting equivalent deposition of GOX solution on rGO coated pet it kept into Spin coating machine after spinning of the substrate it was kept on Hot plate for evaporating the solvent after doing the all process 1L layer rGO_GOX coated pet substrate was prepared. Then doing the same process we have prepared 2 and 3 layers of rGO_GOX coated pet substrate.

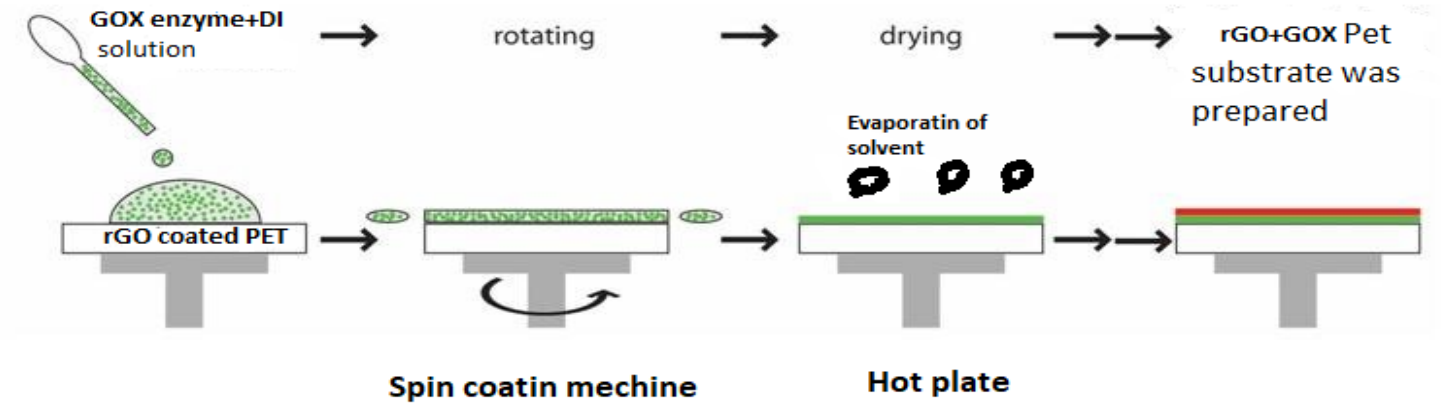


FIG 6.3:Diagram of rGO_GOX coated PET substrate Fabrication process

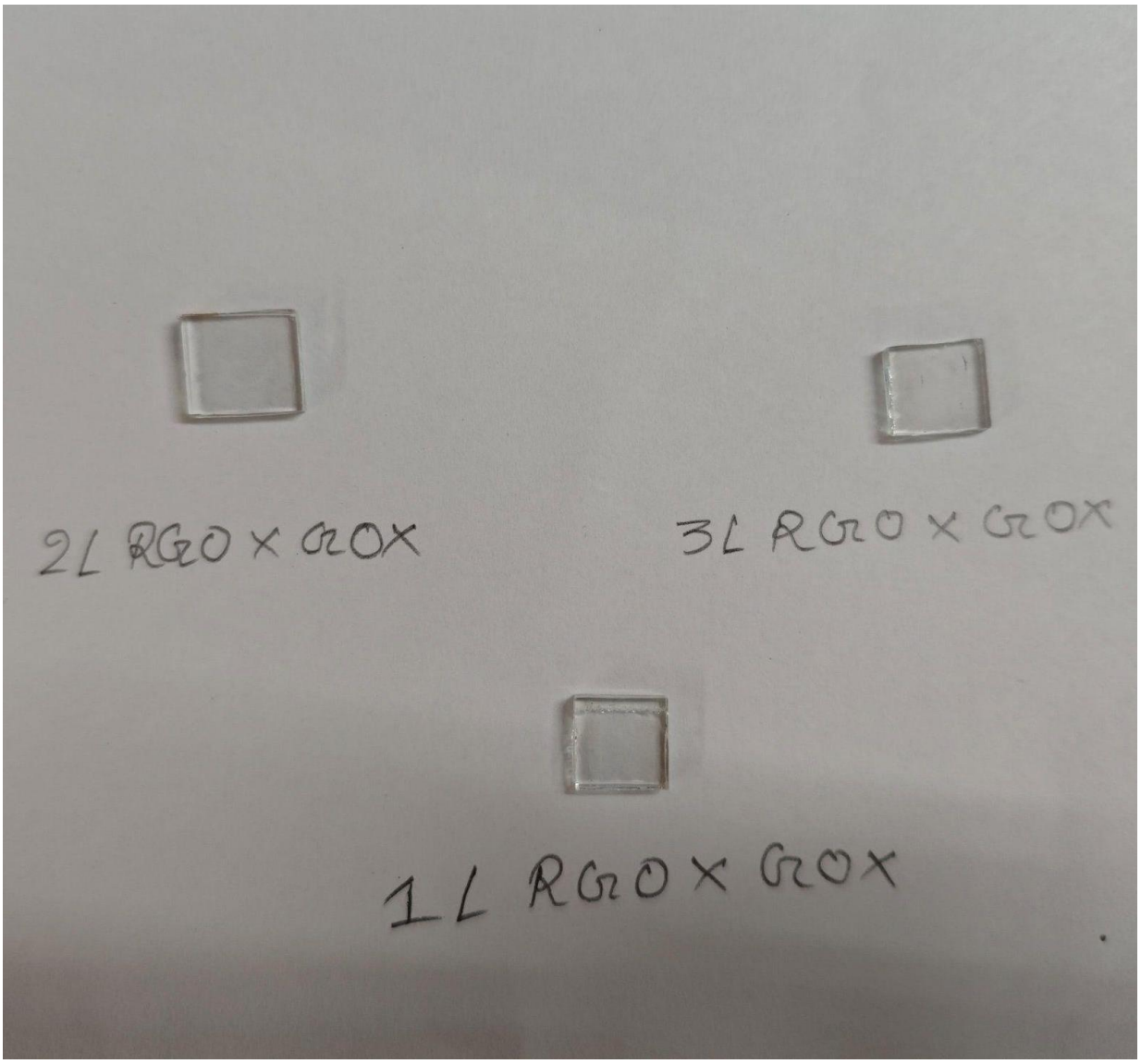


***Fig 6.4 :*Digital photograph of Multiple layer rGO_GOX based PET substrate**

References:

[1] Barth, S.; Hernandez-Ramirez, F.; Holmes, J. D.; Romano- Rodriguez, A. Prog. Mater. Sci.2010, 55, 563.73

[2] Lieber, C. M.; Wang, Z. L. MRS Bull. 2007, 32, 99.

[3] Hayden, O.; Agarwal, R.; Lieber, C. M. Nat. Mater. 2006, 5, 352.

[4] Fan, Z.; Ho, J. C.; Jacobson, Z. A.; Razavi, H.; Javey, A. Proc. Natl. Acad. Sci. U.S.A. 2008,105, 11066. [5] Soci, C.; Zhang, A.; Bao, X.-Y.; Kim, H.; Lo, Y.; Wang, D. J. Nanosci. Nanotechnol. 2010, 10, 1430.

[6] Fischer, . E.; Alem n, B. J.; Tao, S. L.; Daniels, R. H.; Li, E. M.; B nger, M. D.; Nagaraj, G.;Singh, P.; Zettl, A.; Desai, T. A. Nano Lett. 2009, 9, 716.

[7] Snyder, G. J.; Toberer, E. S. Nat. Mater. 2008, 7, 105.

[8] Chan, C. K.; Peng, H.; Liu, G.; McIlwrath, K.; Zhang, X. F.; Huggins, R. A.; Cui, Y. Nat.Nanotechnol. 2008, 3,31.

[9] Liu, E.-S.; Nah, J.; Varahramyan, K. M.; Tutuc, E. Nano Lett. 2010, 10, 3297.

[10] Awschalom, D. D.; Flatte, M. E. Nat. Phys. 2007, 3, 153.

[11] Gould, C.; Pappert, K.; Schmidt, G.; Molenkamp, L. W. Adv. Mater. 2007, 19, 323.

[12] International Technology Roadmap for Semiconductors: 2010 Update Overview;International Technology Roadmap for Semiconductors, 2010.

[13] Ford, D. Semiconductor Revenue Expands by Record Margin in 2010, IHS iSuppli, 2010.Available online: www.isuppli.com.

[14] J. de Boor , N. Geyer , J. V. Wittemann , U. Gösele , V. Schmidt , Nanotechnology 2010 ,21 , 095302.

[15] Y. Harada , X. L. Li , P. W. Bohn , R. G. Nuzzo , J. Am. Chem. Soc. 2001 , 123 , 8709 .

Chapter-7

Results and Discussion



In this chapter, different types of material characterization techniques for hydrothermally synthesized reduced Graphene Oxide (rGO) and metal assist-chemically etched silicon nanowires (SiNWs) have been discussed intensively. These various kinds of characterization techniques include morphological characterization & analysis; crystallographic characterization & analysis and optical or spectroscopic characterization & analysis. Apart from these techniques, to investigate the capacity and efficiency of the final devices, electrochemical and electrical characterization techniques are also being performed thoroughly.

• Morphological Characterization & analysis:

This thesis work involves mainly two types of morphological characterization for the two different samples such as rGO and SiNWs. These are field emission scanning electron microscopy (FESEM) and high-resolution transmission electron microscopy (HRTEM). The FESEM image describes the basic morphological structure of the nanoparticles or nanosheets in the range of 500 nm to 5 μm. Whereas, the HRTEM image provides information about the morphological insights of the nanoparticles such as porosity, length of nanorods etc in the range of 20 nm to 100nm.

• Field Emission Scanning Electron Microscopy (FESEM) of N doped rGO:

Reduced graphene oxide has almost the same morphology as graphene oxide or graphene which refers to the nano-structure of 2D nanomaterials. Their primary morphological structure imitates a sheet-like or layered structure. Here, a crust of thin layers can be seen in NORG- 6h FESEM images [fig (a) & fig (b)] [1]. As the time is low for this synthesis process, the reduction is comparatively low which is resulting in small broken thin layers of N-rGO. Now, in the case of NORG-12h [fig (c) & fig(d)], the layers are stacked one upon one and have long sheets compared to NORG-6h[2].

Fig 8.2 (c, d). FESEM image of NORG-12h

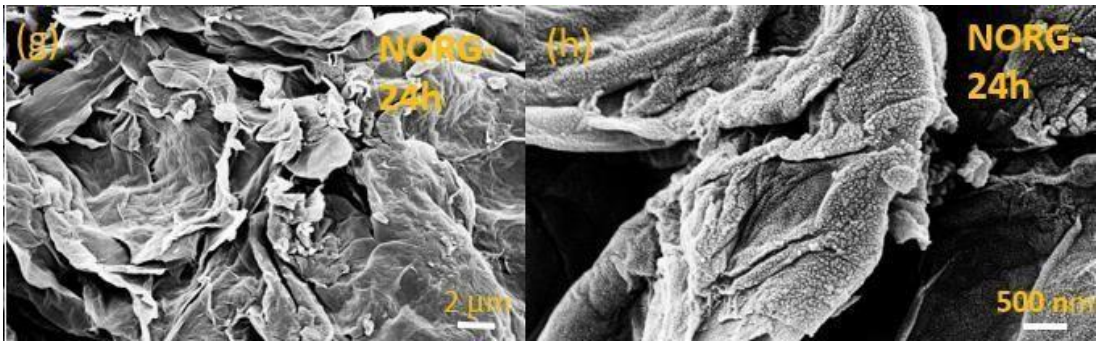


Fig 7.1 (h). FESEM image of NORG-18h & NORG-24h

On the other hand, from the FESEM images of NORG-18h [fig (e) & fig (f)], it is evident that with time the reduction is increasing and resulting in crushed long strains of layered N doped rGO. From fig(f), it can be seen that the aggregation of the layers has been increased in NORG-18h compared to NORG-6h and NORG-12h. Finally, from the NORG-24h [fig (g) & fig (h)] FESEM images, it is clear that with time the reduction had been increased and resulted in large, mostly uniform and unbroken layers of N-doped rGO. Fig (g) provides the confirmation of successful preparation of the best thin layered N doped rGO among the other samples i.e., NORG-6h, NORG-12h & NORG-18h [7].

- **Crystallographic Characterization & Analysis:**

To confirm the crystallographic nature such as crystal structure, interplanar spacing, lattice structure etc. it is very important to perform X-Ray Diffraction (XRD) for the samples. For this project work, XRD had been conducted for hydrothermally synthesized reduced graphene oxide. Here, an illustrative and comparative study of XRD analysis has been carried out and discussed below for NORG-6h, NORG-12h, NORG-18h and NORG-24h.

X-Ray Diffraction Analysis (XRD):

The XRD tool is being operated on the basic principle of Bragg's law of diffraction. It offers information about the crystal type of the material such as amorphous or crystalline structure and the interlayer spacing in between two layers of the material. In this project work, at first, the peak of XRD plots of every sample has been compared with JCPDS database to confirm if the produced material is reduced graphene oxide or not [9]. The average peak angle (2 theta) is equivalent to the JCPDS database record to confirm the products are rGO only. From the below graph, it is also confirmed from the hump or broadness of the peak that these materials are amorphous in nature [12].

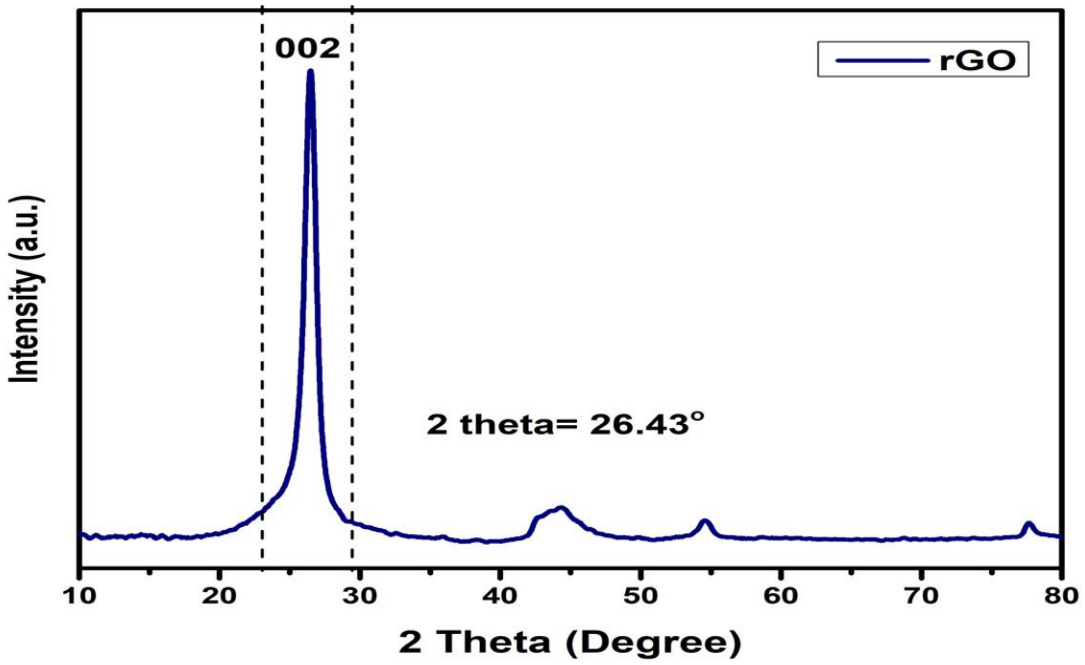


Fig 7.2 XRD analysis of rGO

XRD analysis of rGO:

The provided graph appears to be an X-ray diffraction (XRD)

Pattern for reduced graphene oxide (rGO).Here is a detailed analysis:

XRD pattern Overview:

The XRD pattern displays the intensity (in arbitrary units) on the y-axis versus the 2 theta angle on the x-axis.

The graph shows a distinct peak labeled “002” at 2 theta =26.43˚.

Peak Analysis:

Major Peak: There is a prominent peak labeled “002” at 2 theta= 26.43˚.This peak corresponds to the (002) plane of the rGO structure .

The sharpness and position of this peak are indicative of the degree of reduction and the quality of the graphene sheets .

Minor Peak: There are smaller peaks at higher angles, but the main focus is on the dominant peak

Interpreting the (002) peak:

The (002) peak at 26.43˚is characteristic of the graphitic structure in rGO. It corresponds to the interlayer Spacing(d-spacing) between graphene sheets.

Using Bragg’s Law,

$n\lambda = 2d\sin\Theta$

The d spacing can be calculated,

$d = n\lambda / 2\sin\Theta$

Where, n=1(first order diffraction),

$\lambda = 1.54$Å (the wavelength of the X-ray source, typically Cu ką radiation)

Θ=13.215˚(half of 26.43˚)

So, d = 1.54/2*sin(13.215)

d = 3.38 Å

Significance of the d-Spacing:

The calculated d-spacing (~3.38 Å) is consistent with the typical interlayer distance in reduced graphene oxide, which is smaller than that of graphite oxide (~6-7 Å) due to the removal of oxygen-containing groups and the restoration of the graphitic structure.

Overall Structural Information:

The sharp and intense peak indicates that the rGO sample has well-defined, crystalline graphitic layers.

The presence of other minor peaks suggests there might be other phases or less ordered regions in the sample.

Applications and Implications:

Understanding the XRD pattern of rGO is crucial for applications in energy storage, sensors, and other fields where the structural properties of graphene materials play a critical role.

The quality and properties of rGO can be tailored by controlling the reduction process and starting materials, as reflected in the XRD pattern.

In summary, the provided XRD pattern shows that the rGO sample has a dominant (002) peak at 26.43°, indicating good quality graphitic layers with an interlayer spacing of approximately 3.38 Å. This information is essential for assessing the structural properties and potential applications of the rGO material.

- **Spectroscopic Characterization & Analysis:**

➢ **UV-Vis Spectroscopy of rGO:**

Ultraviolet-visible spectroscopy is reflectance spectroscopy and absorption spectroscopy consisting of the ultraviolet and the adjacent full visible regions of electromagnetic spectrum, i.e., it uses light in the visible and the adjacent ranges. The reflectance or absorption in the visible range directly affects the perceived colors of the chemicals involved. In this region of the spectrum. atoms and molecules undergo electronic transitions. Absorption spectroscopy is complementary to fluorescence spectroscopy. Fluorescence deals with the transition from the excited state to the ground state whereas absorption deals with the transition from ground state to the excited state.

Spectroscopic analysis is usually done in solutions but solids and gasses may also be studied using this. It can also be used to determine kinetics or the rate of a chemical reaction

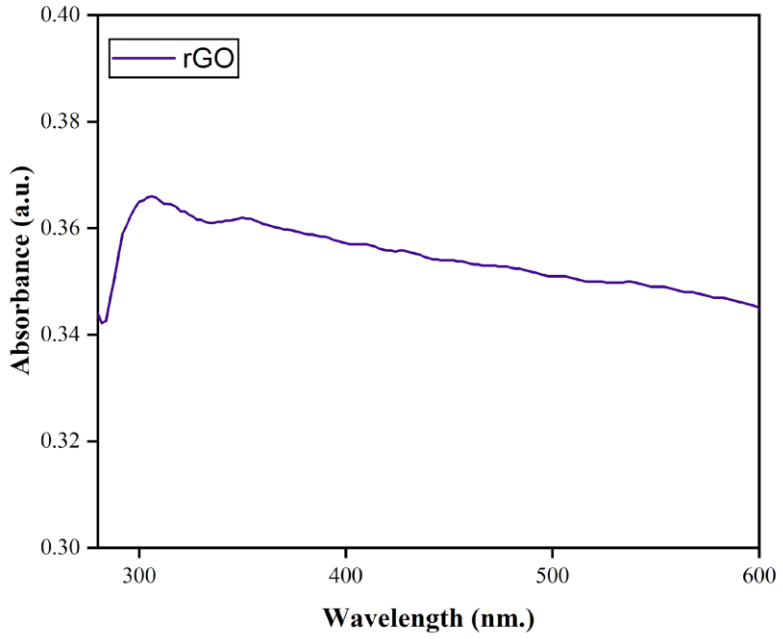


Fig 7.3 UV-Vis analysis of rGO

The provided graph displays the UV-Vis absorbance spectrum of reduced graphene oxide (rGO).Below is a detailed analysis of the graph.

X-Axis(wavelength in nm):The wavelength range is from 300 nm to 600 nm.

Y-Axis (Absorbance in a.u):The absorbance range is from 0.30 to 0.40 arbitrary units(a.u).

Plot Characteristics:

Line color and Label :The plot line is purple ,labeled “rGO” in the legend.

Observations

Initial Absorbance (300 nm): The absorbance starts at just above 0.3 a.u around 300 nm.

Peak formation :There is a slight peak in absorbance occurring around 320 nm, reaching slightly above 0.36 a.u.

General trend: After the peak , the absorbance decreases gradually with slight fluctuations until it reaches around 0.33 a.u at 600 nm.

Smoothness: The overall curve is relatively smooth with no sharp spikes , indicating consistent absorbance characteristics across the measured wavelength.

Analysis:

Peak near 320 nm: This peak could correspond to the characteristics π_ π* transition as the wavelength increases.

The UV-Vis spectrum of rGO shows a characteristics peak around 320 nm, which is typical for the π_ π* transition in graphene based materials.The absorbance decreases slightly over the measured range, which aligns with typical behavior for rGO as the energy with increasing wavelength.

FOURIER TRANSFORM INFRA-RED SPECTROSCOPY (FTIR) of rGO:

The image is an FTIR (Fourier-transform infrared spectroscopy) spectrum, which shows the transmittance of a sample across a range of wavenumbers (cm^-1).The peaks and their corresponding wavenumbers indicate the presence of specific functional groups in the sample.

Here is a detailed analysis of the FTIR spectrum:

3440 cm^-1 (O-H stretch): The broad peak around 3440 cm^-1 corresponds to the O-H stretching vibration, This is typically indicative of hydroxyl groups (alcohols and phenols) or moisture content in the sample.

2944 cm^-1 (C-H stretch): is associated with the C-H stretching vibration, which is characteristic of aliphatic hydrocarbons (alkanes).

The peak at 2326 cm^-1: corresponds to the C≡N stretching vibration, indicating the presence of nitriles (cyano groups).

1745 cm^-1 (C=O Stretch)

The peak at 1745 cm^-1: is due to the C=O stretching vibration. This is commonly seen in carbonyl groups, such as those in aldehydes, ketones, carboxylic acids, and esters.

1647 cm^-1 (C=C Stretch): The peak at 1647 cm^-1 is indicative of C=C stretching, which is characteristic of alkenes or aromatic rings.

1440 cm^-1 (C-O-C Stretch): The peak at 1440 cm^-1 corresponds to the C-O-C stretching vibration, suggesting the presence of ether linkages or epoxy groups.

1300 cm^-1 (C-O Stretch)

The peak at 1300 cm^-1: is associated with the C-O stretching vibration, often seen in alcohols, ethers, carboxylic acids, and esters.

These peaks provide information about the chemical bonds

and functional groups present in the sample. The specific functional groups identified include hydroxyl (O−H), aliphatic hydrocarbons (C−H), nitriles (C≡N), carbonyl groups (C=O), alkenes/aromatic rings (C=C), and ether/epoxy (C−O−C, C−O).

The colors highlighted in the background of the graph (yellow, green, blue, pink, brown, and light blue) are used to emphasize the regions corresponding to these functional groups for easier visualization and identification.

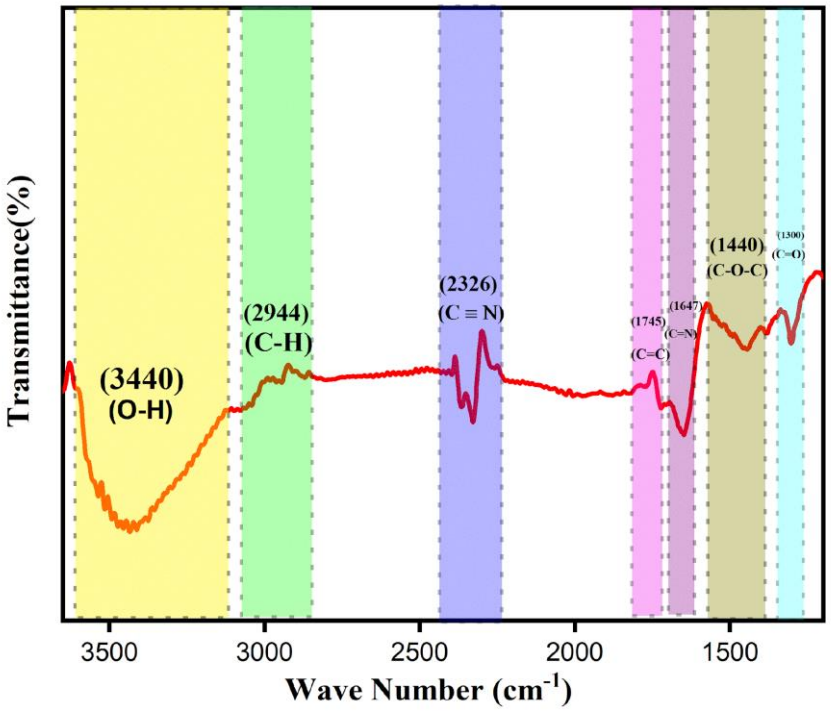


Fig 7.4. FTIR plot of rGO-24h.

References:

1. J. Hou, Y. Shao, M. W. Ellis, R.B. Moore, B. Yi, Graphene-based electrochemical energy conversion and storage: fuel cells, supercapacitors and lithium ion batteries, Phys. Chem. Chem. Phys. (13) (2011) 15384-15402.

2. Z. Peng, H. Yang,Synthesis and oxygen reduction electrocatalytic property of Pt-on-Pd bimetallic hetero nanostructures, J. Am. Chem. Soc. (131)(2009) 7542–7543.

3. J. D. Zhang, M. R. Vukmirovic, Y. Xu, M.Mavrikakis, R.R. Adzic, Controlling the catalytic activity of platinum-monolayer electrocatalysts for oxygen reduction with different substrates, Angew. Chem., Int. Ed. (44)(2005) 2170–2173.

4. G. Wu, K. L. More, C.M. Johnston, P. Zelenay, Polymer wrapping technique: an effective route to prepare Pt nanoflower/carbon nanotube hybrids and application in oxygen reduction Science,(332)(2011) 443–447. 4. W. Yang, Y. Wang, J. Li, X. Yang, Polymer wrapping technique: an effective route to prepare Pt nanoflower/carbon nanotube hybrids and application in oxygen reductionEnviron. Sci, (3)(2010) 144–149.

5. S. Wang, S. P. Jiang, X. Wang, Polyelectrolyte functionalized carbon nanotubes as a support for noble metal electrocatalysts and their activity for methanol oxidation Energy Nanotechnology,(19)(2008) 265601.

6. S. Wang, F. Yang, S. P. Jiang, S. Chen, X. Wang, Tuning the electrocatalytic activity of Pt nanoparticles on carbon nanotubes via surface functionalization, Electrochem. Commun.(12) (122010) 1646–1649.

7. S. Y. Wang, X. Wang, S.P. Jiang, PtRu nanoparticles supported on 1-aminopyrenefunctionalized multiwalled carbon nanotubes and their electrocatalytic activity for methanol oxidation, Langmuir (24)(2008) 10505–10512. 19

8. S. Y. Wang, N. Kristian, S. P. Jiang, X. Wang, Controlled synthesis of dendritic Au@ Pt core–shell nanomaterials for use as an effective fuel cell electrocatalyst, Nanotechnology, (20)(2009) 25605.

9. S. Wang, S.P. Jiang, T.J. White, X. Wang, Synthesis of Pt and Pd nanosheets on multiwalled carbon nanotubes as potential electrocatalysts of low temperature fuel cells, Electrochim. Acta. (55)(2010) 7652–7658.

10. C. Goswami, K. K.Hazarika, P.Bharali, Transition metal oxide nanocatalysts for oxygen reduction reaction,Materials Science for Energy Technologies, 2018.

11. L. Li, J. He, Y. Wang, X. Lv, X. Gu, P. Dai, D. Liu, X. Zhao,Metal–organic frameworks: a promising platform for constructing non-noble electrocatalysts for the oxygen-reduction reactionJ. Mater. Chem. A(7)(2019) 1964-1988.

12.S. J. Rowley Neale, J. M. Fearn, D. A. Brownson, G. C. Smith, X. Ji, C. E. Banks,molybdenum disulphide (2D-MoS 2) modified electrodes explored towards the oxygen reduction reaction, Nanoscale (8)(2016) 14767-14777.

13. C. Hu, Y. Zhou, R.Ma, Q. Liu, J. Wang,Reactive template synthesis of nitrogen-doped graphene-like carbon nanosheets derived from hydroxypropyl methylcellulose and dicyandiamide as efficient oxygen reduction electrocatalysts, J. Power Sources (345)(2017) 120-130.

14. W. Wei, Y. Tao, W. Lv, F.Y. Su, L.Ke, J. Li, D. W. Wang, B. Li, F. Kang, Q. H. Yang,Unusual high oxygen reduction performance in all-carbon electrocatalysts, Sci, Rep (4)(2014) 6289.

15. T. Chen, L. Dai, Carbon nanomaterials for high-performance supercapacitors, Mater. Today (16) (2013), 272-280.

16. A. K. Geim, K. S. Novoselov, The rise of graphene, Nat. Mater.(6) (2007)183–191. 20

17. K. S. Novoselov, A. K.Geim, S. V.Morozov, D. Jiang, Y. Zhang, S. V.Dubonos, I. V. Grigorieva, A. A. Firsov, Electric field effect in atomically thin carbon films,Science (306)(2004) 666–669.

18.K. S. Kim, Y. Zhao, H. Jang, S. Y. Lee, J. M. Kim, K. S. Kim, J. H.Ahn, P. Kim, J. Y. Choi, B. H. Hong, Large-scale pattern growth of graphene films for stretchable transparent electrodes, Nature(457)(2009) 706-710.

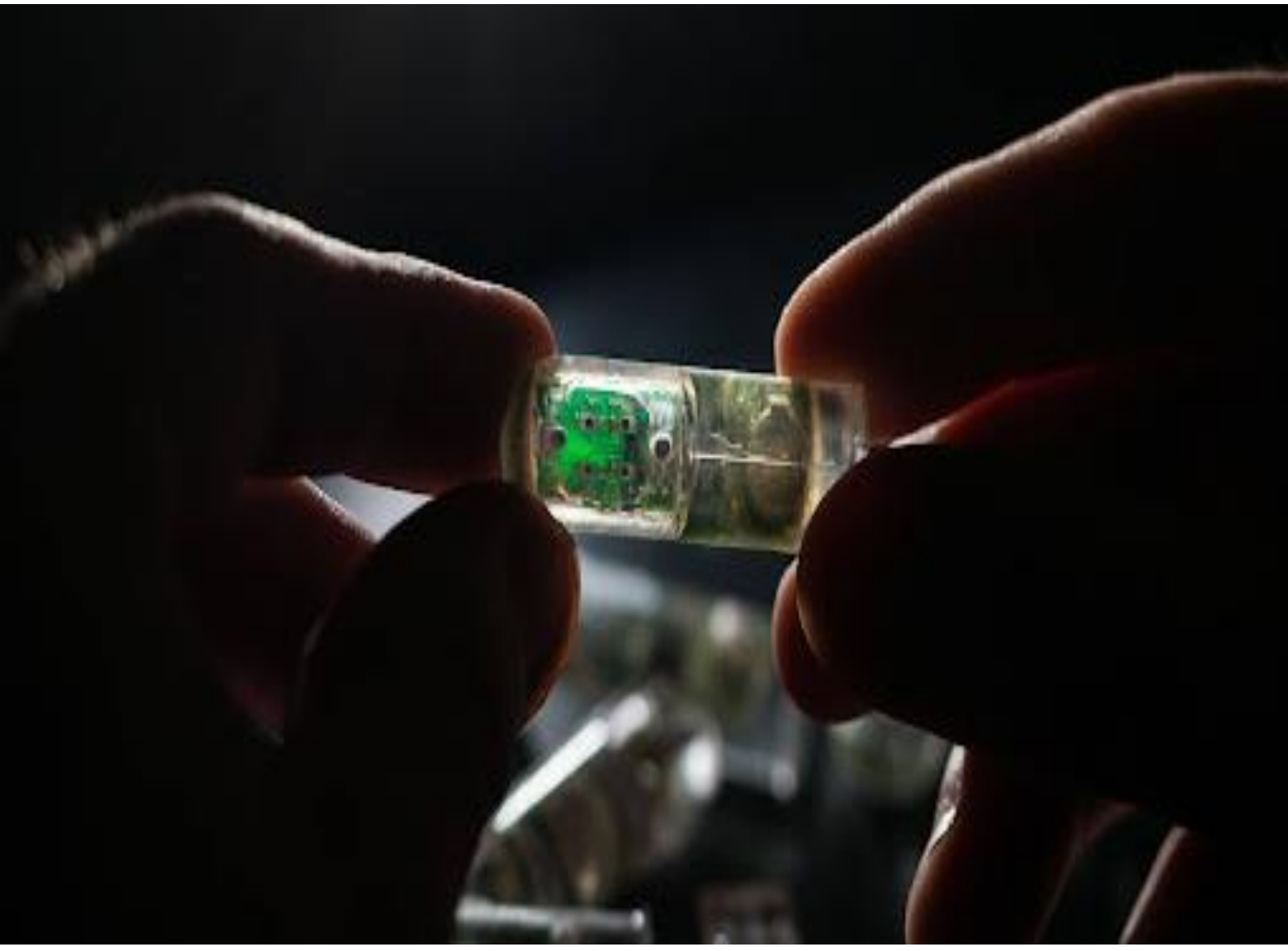
19. K. V. Emtsev, A. Bostwick, K. Horn, J. Jobst, G. L. Kellogg, L. Ley, J. L. McChesney, T. Ohta, S. A. Reshanov, J. Röhrl, E. Rotenberg, Towards wafer-size graphene layers by atmospheric pressure graphitization of silicon carbide, Nat.Mater.(8) (2009) 203.

20. C. Berger, Z. Song, X. Li, X. Wu, N. Brown, C. Naud, D. Mayou, T. Li, J. Hass, A. N. Marchenkov, E. H. Conrad, Electronic confinement and coherence in patterned epitaxial graphene,Science312 (2006)1191-1196.

Chapter-8

Device performance

(Glucose sensor)



- **I-V Analysis:**

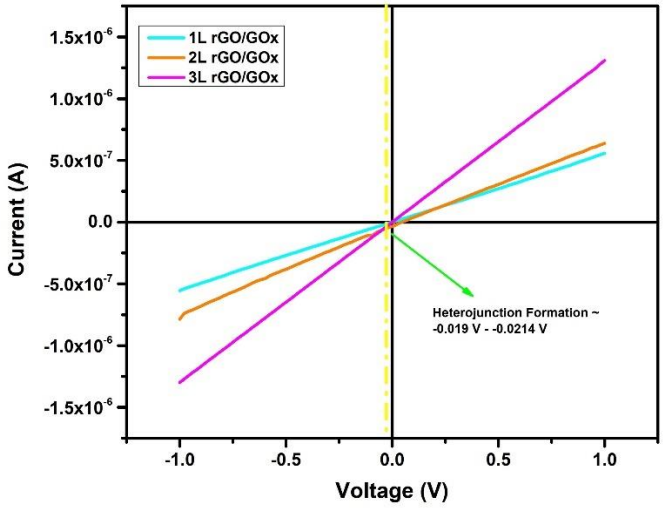


Fig 8.1 1L,2L,3L rGO

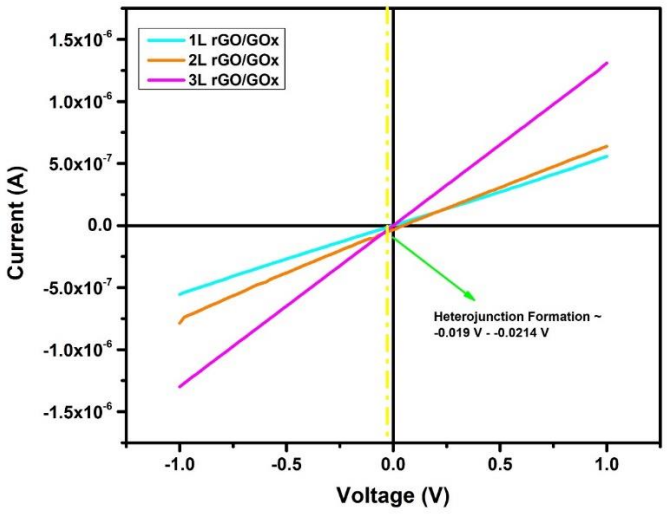


FIG 8.2 1L rGO/GOX, 2L rGO/GOX, 3L rGO/GOX.

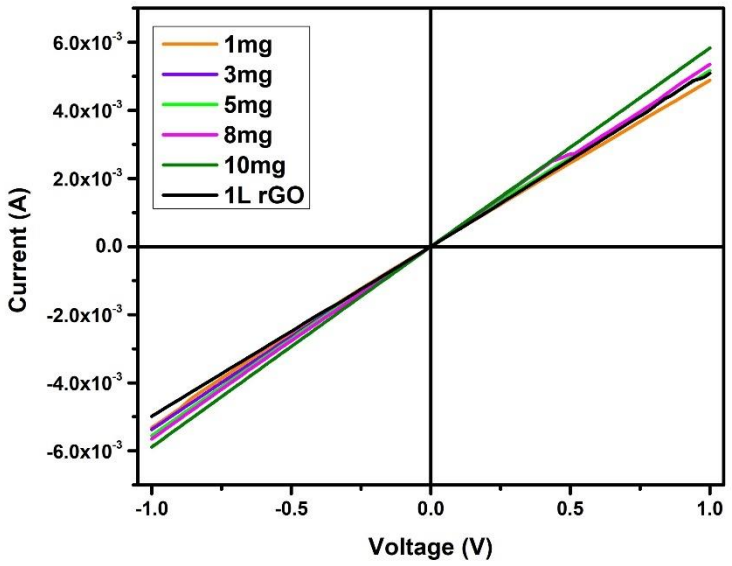


Fig 8.3 1L rGO following glucose concentration

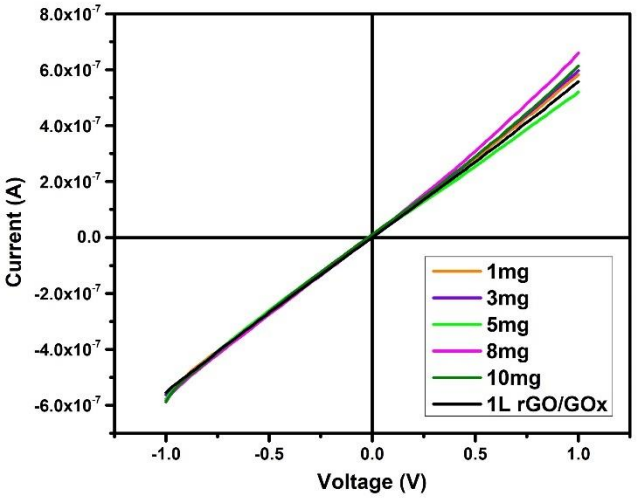


FIG 8.4 1L rGO+GOX following glucose concentration

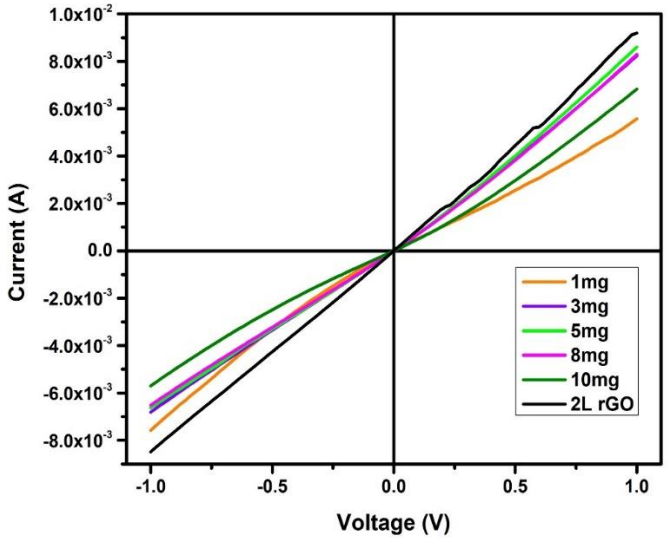
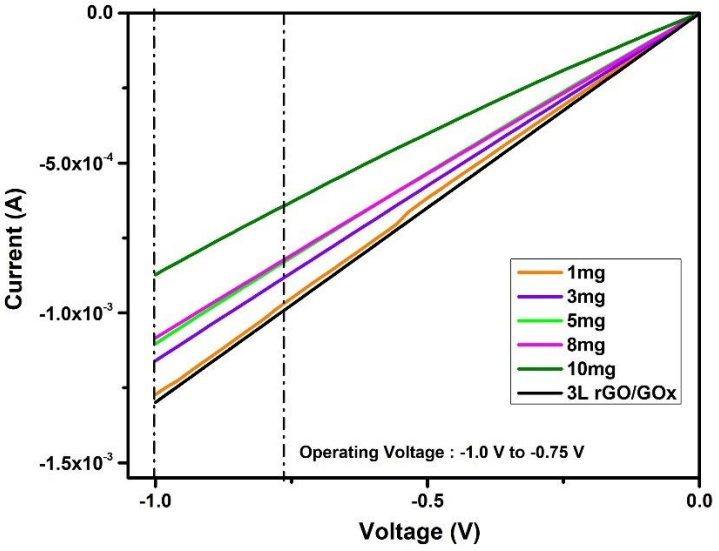


Fig 8.5 2L rGO following glucose concentration



Fg8 .6 3L rGO+GOX following glucose concentration

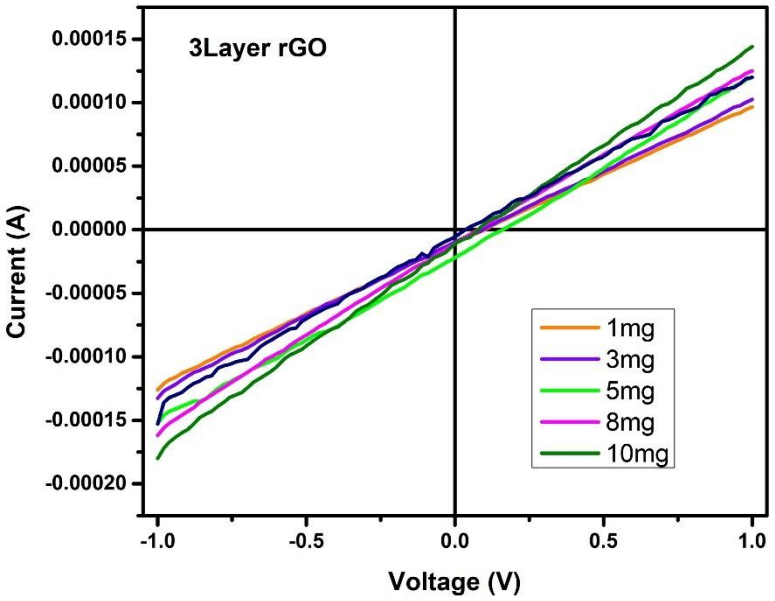


Fig 8.7 3L rGO following glucose concentration

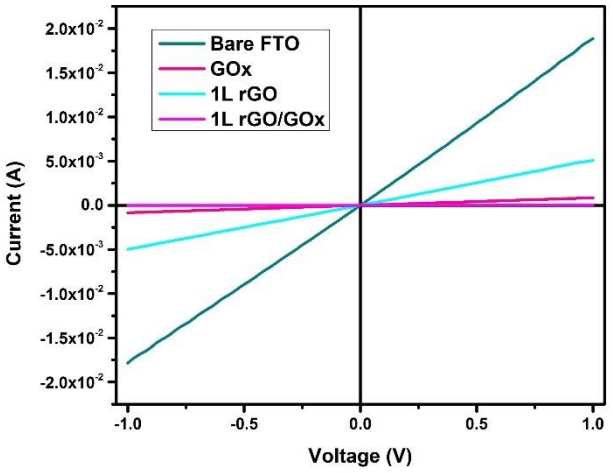


Fig 8.8 Bare FTO+GOX+1L rGO+1L rGO/GOx

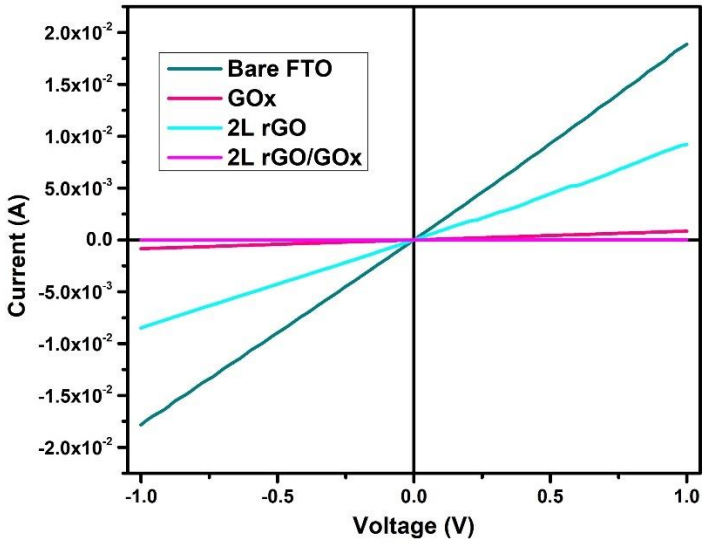


Fig 8.9 Bare FTO+GOX+2L rGO+2LrGO/GOx

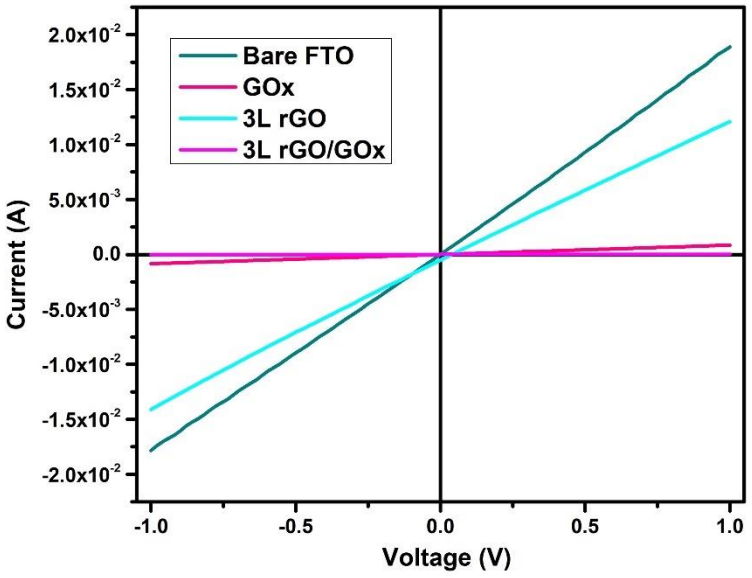


Fig 8.10 Bare FTO+GOx+3L rGO +3L rGO/GOX

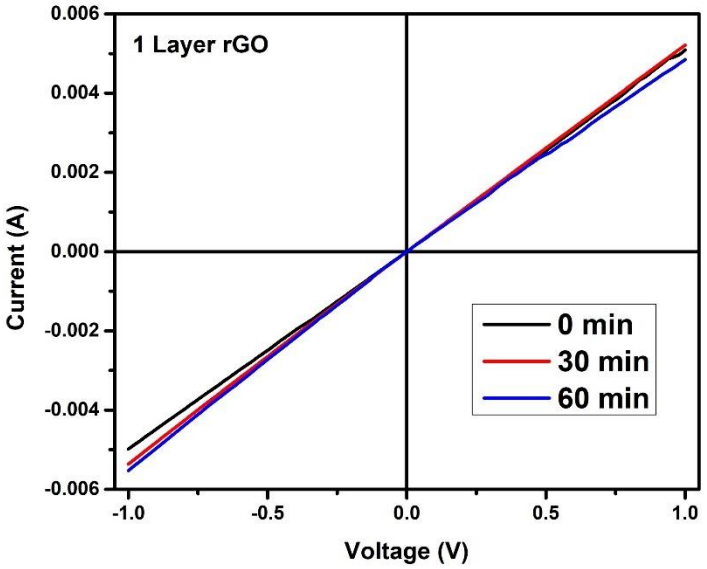


FIG 8.11 Retention time 0 min,30 min,60min 1L rGO

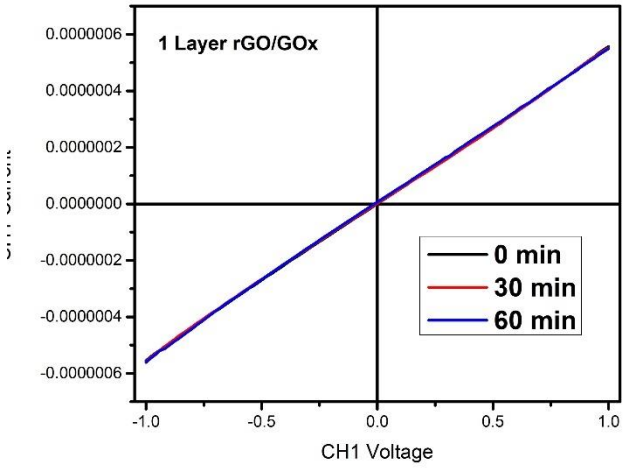


FIG 8.11 Retention time 0 min,30 min,60min 1L rGO/GOx

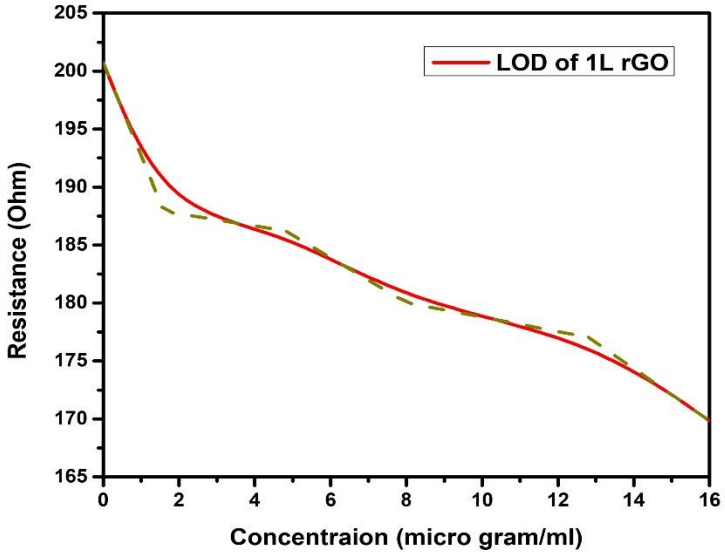


Fig 8.13 Load 1L rGO

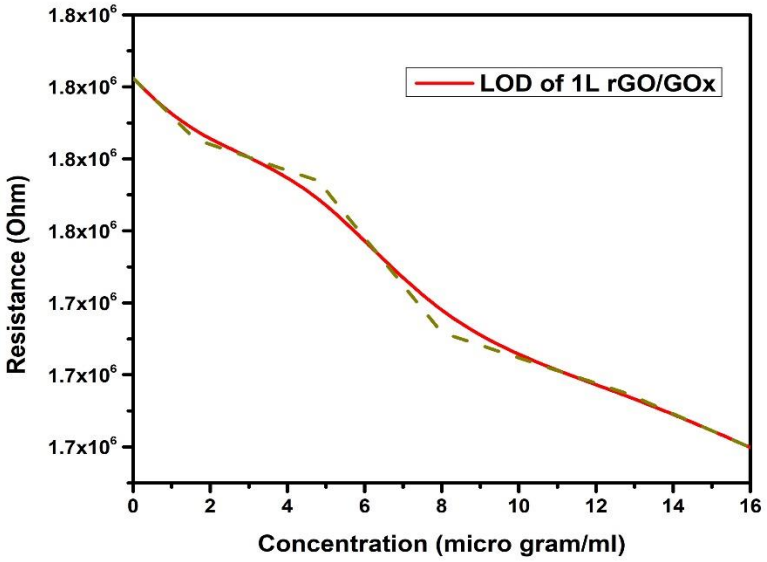


Fig 8.14 Load 1L rGO/GOX

Chapter-9

Conclusion



• Conclusion:

The study successfully synthesized porous nitrogen-doped reduced graphene oxide (N-rGO) using a hydrothermal method, following the prior preparation of graphene oxide (GO) through a modified Hummer's method. The crystallinity and phase were confirmed using XRD tools, and morphological analysis through FESEM and HRTEM revealed a flake-like structure and porous nature of the reduced graphene oxide (rGO). UV-vis comparison of band gaps between silicon nanowire and rGO identified the latter as the most suitable for fabricating photodetectors.

This work describes synthesizing porous nitrogen-doped reduced graphene oxide (N-rGO) via hydrothermal synthesis and it's application as non- enzymatic glucose sensor . Before that, graphene oxide (GO) was prepared using a modified version of Hummer's process. The crystallinity and phase have been verified with an XRD device. Morphological analysis using FESEM images confirms the porous nature. Conversely, comparisons of their UV-vis have been done to help determine the band gaps between GO and rGO. In this project, electrical (resistive) biosensor for glucose monitoring has been experienced. A comparison study of different layers, enzymatic interaction and their out has been carried for the rGO based devices. Here, alpha- glucose has been tested with the biosensor. After a layer-dependent experiment, it can be expressed from the I-V analysis 1layer rGO device has shown a better response than GOx+rGO-coated all devices.1L rGO-coated device also gives better response than 1L GOx+rGO and from LOD curve it can be clearly stated that 1 layer rGO coated device has better sensibility in all aspect..